Naval Research Reviews

Office of Naval Research
Two / 1987
Vol XXXIX

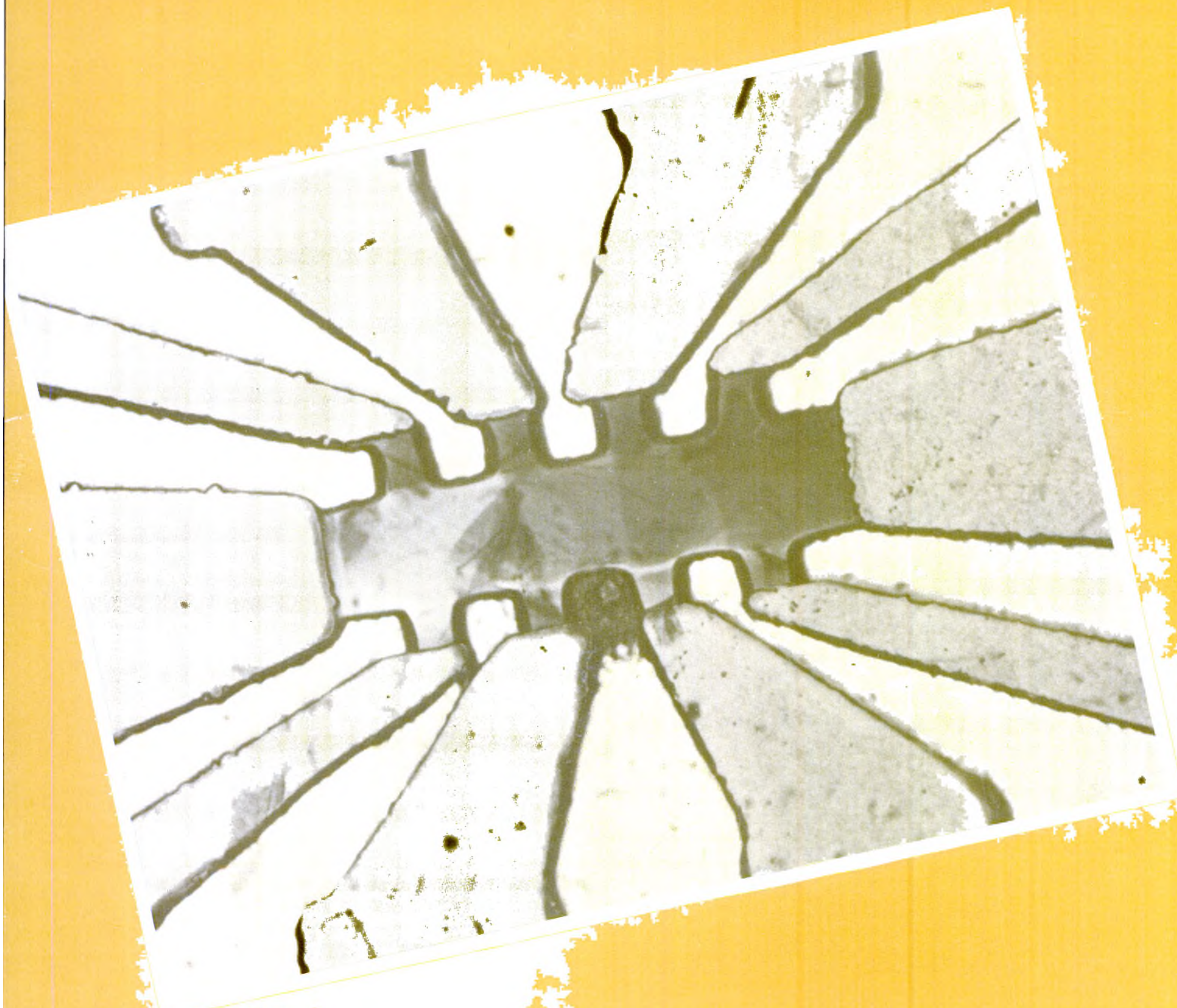

Surf Zone and Beach Dynamics

Along shore effects of wave motions

The United States Marine Corps and Navy SEALs know full well the importance of understanding how nature operates in the beach/surf zone. For a quarter century, the Office of Naval Research (ONR) has been the forefront agency in supporting science that reveals the intricacies of this dynamic, sometimes violent environment. The most surprising result has been the realization and confirmation that the most important waves in the surf zone are not necessarily the obvious wind waves which break at the shore, but rather long-period (30 seconds – 5 minutes period) which move *lateral* to the shore. These are trapped by nearshore topography and have maximum energy in the surf zone. First proposed by Walter Munk in 1948, 'edge waves' became firmly validated in nearshore hydrodynamics after more than a decade of research, mid '60s to early '80s. This research was led primarily by scientists of Scripps Institution of Oceanography under ONR support.

This understanding is essential for the accurate prediction of beach changes, during and after storms. These predictions are required for precise definition of naval landing conditions and the construction of temporary harbor facilities required for getting heavy equipment ashore, after the initial landings, on open coasts.

Naval Research Reviews

Office of Naval Research
Two / 1987
Vol XXXIX

Articles

Departments

About the Cover

A quantum state transfer device fabricated at the Naval Research Laboratory on an artificially structured semiconductor by molecular beam epitaxy. This device demonstrates the phenomenon of resonant tunneling between adjacent semiconductor quantum energy wells. This mechanism may find application in the next generation of ultra high speed device technologies which may switch in a tenth of one picosecond. (See article on page 2)

Naval Research Reviews publishes articles about research conducted by the laboratories and contractors of the Office of Naval Research and describes important naval experimental activities. Manuscripts submitted for publication, correspondence concerning prospective articles, and changes of address, should be directed to Code OPARI, Office of Naval Research, Arlington, Va. 22217-5000. Requests for subscriptions should be directed to the Superintendent of Documents, U.S. Government Printing Office, Washington, D.C. 20402. *Naval Research Reviews* is published from appropriated funds by authority of the Office of Naval Research in accordance with Navy Publications and Printing Regulations. NAVSO P-35.

FUTURE PROSPECTS FOR ELECTRONICS IN NANOMETER STRUCTURES

By Gerald M. Borsuk
Naval Research Laboratory

The silicon transistor and its incorporation into ever more complex and dense planar very large scale digital integrated circuits (VLSI) has been the key element driving rapid advances in information, computer and electronic technologies. These high technologies have been action multipliers for economic growth, productivity enhancement, and standard of living improvements in the second half of the 20th century. However, there are signs that this extraordinary pace in traditional microelectronics will be slowing. This paper will examine the factors which influence near term technological development and explore the science and technology issues that will be necessary to set electronics on another revolutionary expansion as the 21st century is approached.

Background

The scientific foundation of these electronic advances has been the uncovering of the fortuitous properties of crystalline silicon material. Silicon can be grown with high purity and low bulk defects, has the relatively advantageous electronic bandgap of 1.12 eV, good thermal conductivity, and allows the growth by thermal oxidation of high quality silicon dioxide thin films with low interface defect density. The important technological elements that have enabled the drive to increased density of active devices on a single monolithic substrate has been the ability to use optical lithography as the patterning tool, batch fabrication processes, and the advantageous physical attributes of scaled down device dimensions. Although other more optimal models exist, the constant electric field model for MOSFET scaling can be used as an example of the attributes of scaling to smaller dimensions. Applying this model shows that as device geometries are reduced by a scaling factor(>1), the number of devices per unit area is increased by the square of this scaling factor, delay time between active devices is reduced to first order by the scaling factor, and power dissipation is reduced by the square of the scaling factor. The resulting power-delay product is reduced by the cube of the scaling factor. As an example, scaling down transistor feature size from 2 micrometers to 1 micrometer results in almost an order of magnitude improvement in power-delay product. These advantageous scaling attributes have been the driving force behind Moore's law which states that monolithic integrated circuit density increases by about a factor of four every two years. Remarkably, Moore's law has accurately predicted the pace of increased monolithic circuit integration since the early 1960's. This relationship between integrated circuit chip density and year in which the chip became commercially available is shown in Figure 1 for dynamic random access memories (DRAMs). The plots are similar for other integrated circuit types such as those for logic. Significant impediments to maintaining the historical rate of miniaturization exist. For near term conventional technologies, these impediments include the limitations imposed by the failure of device scaling, excessive interchip signal propagation delays between gates due to architecture dependent interconnections; the difficulties in maintaining acceptable yields as material and process-related defects play an increased role in small geometry structures; the high cost of capital equipment, particularly in lithographic tools necessary to manufacture the ICs; and the impending limitations in time efficient design of new generations of these circuits. Not withstanding these difficulties, projections for the next seven years envision the continued pace of miniaturization as shown in Table 1.[1] These levels of integration in silicon VLSI are likely to be achieved because scaling to the necessary device feature size of about 0.2 micrometers will still result in advantageous device and circuit properties such as higher speed and manageable power dissipation on the chip level. Reducing feature sizes much below about 0.2 micrometers will introduce significant fundamental problems in the performance of traditional three terminal devices and high density circuits as well as in the processes for low cost fabrication. Fundamental device physics limitations to scaling include drain junction breakdown, hot electron injection into thin gate oxides at the drain, Fowler-Nordheim tunneling through thin gate oxides, resistance of shallow junctions needed to maintain long channel device behavior, and threshold voltage scaling failure due to the difference in work function between gate material and the channel inversion layer. There is, however, significant advantage to be realized by continued miniaturization. Signal propagation delay between gates will decrease because of decreased interconnection length. Increased levels of monolithic integration will be crucial to achievement of higher performance, greater functionality, and increased reliability. Also, new forms of computer functionality, such as associative memory, may open completely new avenues to computer science.

Figure 1

The relationship between dynamic random access memory integrated circuit component density and the year the chip became commercially available.

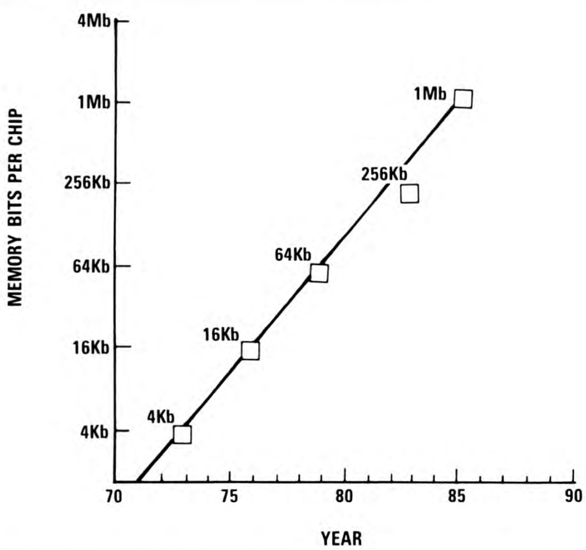

The major research approach to achieving the goals of a new generation of ultra high density nanometric circuits centers upon artificially structured materials. Advances in material growth techniques by molecular beam epitaxy and other methods have produced layers of semiconductor materials one atomic layer at a time with precise control of the number and stoichiometry of these layers. Much has been learned about the electronic properties of these microstructures and many technologically useful applications in photonics and solid state devices have already been found. However, in terms of ultra small features only half of the problem has been solved. Control of the planar dimension to nanometric tolerances will be necessary to fulfill the promise of a new generation of integrated circuits. Therefore monolithic circuits based upon nanometric devices will require advances in material science, specifically in artificially structured crystals; in process science, specifically in the areas of dimensional control and yield; in device physics, specifically addressing low power dissipation, low noise, and minimized parasitics; and in circuit architectures and function, specifically in the area of massively interconnected device functions.

Table 1

Trends in silicon VLSI DRAM Sc.

MEMORY SIZE	FIRST REPORTED	AVAILABLE	FEATURE SIZE
64K	1978	1980	3 MICRONS
256K	1980	1983	1.5 MICRONS
1M	1984	1986	1 MICRON
4M	1986	1988?	1 MICRON
16M	1987*	1990?	∿.5 MICRONS
64M	?	1992?	<0.5 MICRONS
256M**	?	1994?	∿0.25 MICRONS

*REPORTED AT THE FEB. 1987 ISSCC

**SRC GOALS
CMOS
4 LEVEL METAL
50 pS SWITCH DELAY

An important issue to be examined is whether silicon or compound semiconductor materials will evolve as the basis for nanometric technologies of the future. Gallium arsenide and similar compound semiconductors are important electronic materials. These materials form the basis of significant optoelectronic and rf analog technologies in part because of their direct bandgap, high electron mobilities, and lattice matched heterostructure properties. Two important properties of these materials give them a distinct advantage over silicon in the realization of nanometer technologies. First, quantum effects in electronic transport occur in structures with larger dimensions than silicon because the effective mass of electrons in these materials is significantly less than in silicon. Second, the opportunities for making new artificially structured heteroepitaxial thin layered materials with the engineered electronic and opto-electronic properties which give rise to quantum effects are greater because of the lattice matching properties of ternary and quaternary derivatives of the corresponding group III and V elements. However, electronic quantum transport phenomena can be observed in silicon structures.[2] Low temperature silicon deposition by MBE, for example, may produce new avenues for novel silicon based layered devices. However, the amenable manufacturing attributes of silicon will produce tremendous incentive to continue its use regardless of high density circuit maturity. It may be more economical to find new packaging and cooling methods and to improve yield for minimum design rule traditional silicon technologies than to make a major commitment to bring to production emerging nanometric technologies. The rate of scientific progress in the nano-regime over the next five to seven years in materials, processing science, and device physics will be the crucial factors pacing the insertion of nanometric technologies into the market place. These factors are discussed below.

Scientific Progress Required

Materials

The constituent materials important for accessing future nanometrlc e1ectronics are semiconductor bulk crystals, artificially structured materials, and grown or deposited materials that are an integral part of the fabrication process. All of these areas of material science will be important in determining future trends in nanometric devices.

Bulk crystal materials form the host substrate for artificially layered structures. The required physical properties of these substrate materials include low surface dislocation density, lattice parameters that match those of the epitaxial layers, and we11 characterized and controlled defects. Technological requirements include the ability to produce the material in large volume, in large diameter wafers, with well controlled surface topographies, and at low cost relative to the total cost of wafer fabrication. The two most technologically advanced bulk semiconductor materials are silicon and gallium arsenide. Silicon has been and will remain for the next seven to ten years the predominant starting material for digital ultra large scale integration. Most silicon starting material is grown by the Czochralski method. The quality of this material is adequate for present and near term extension of silicon technology. Important impurities in silicon starting material made by the Czochralski method are carbon and oxygen. Although carbon is electrically inactive, its presence is undesirable because it aids the formation of defects. Substantial improvement in the quality of GaAs starting material will be necessary. Specifically, reduction and control of defects will be necessary if this class of compound semiconductor bulk crystal material is to be highly useful for high density nanometric circuits.

Non-equilibrium growth and synthesis techniques have produced new artificially structured epitaxial materials with unique electrical, optical, and mechanical properties. The ability to deposit specific species of atoms or molecules on semiconductor substrates in the thickness of one atomic layer with a given stoichiometry is the essential requirement for electronic materials of the next century. The controllable properties of these artificially structured materials of most value to nanometric electronics are listed in Table 2. The methods used to synthesize these multilayer materials include molecular beam epitaxy (MBE), metal-organic chemical vapor deposition (MOCVD), liquid and solid phase epitaxy, and sputtering and ion beam deposition. Of these approaches, molecular beam epitaxy is used most frequently in research which requires the greatest control over layer interface abruptness. MBE is a low temperature ultra-high vacuum growth method. The major impediment to its use as a production deposition apparatus is the slow growth rate of layers, limited running time between re-charges, and surface oval defects. A photograph of a typical MBE instrument is shown in Figure 2. MOCVD is a low or atmospheric pressure, low temperature method for multi-layer deposition of a broad range of materials. This method holds great promise for economical production of layered starting material for future nanometric electronics because of its capability to deposit thin layers rapidly over large substrate areas including materials, such as refractories, for which MBE is unsuited. Present limitations of MOCVD for large scale production are a lack of suitable metal-organic carrier gases for several technologically important types of impurity dopants, and film contamination by unwanted impurities present in the gas. Research to overcome these limitations is on-going. Environmental pollution and safety are also important issues because of the toxicity several commonly used gases.

Figure 2

A molecular beam epitaxy (MBE) apparatus.

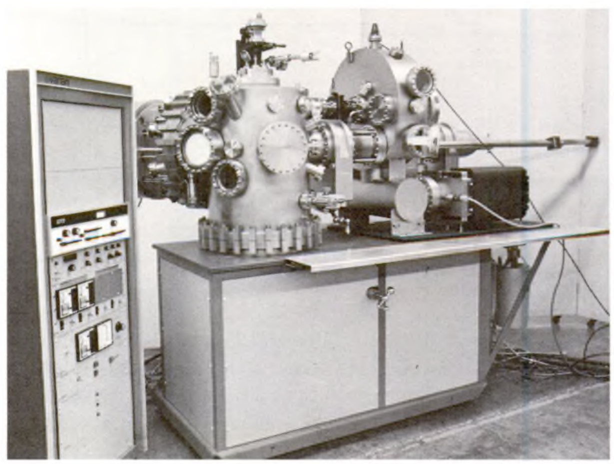

Table 2

Controllable properties of artificially structured materials.

- **EFFECTIVE DIMENSIONALITY**
- **BAND STRUCTURE**
- **BAND GAP**
- **POTENTIAL ENERGY PROFILE**
- **CARRIER CONCENTRATION, MOBILITY, EFFECTIVE MASS**
- **IMPURITY BINDING ENERGY**
- **LATTICE CONSTANT**
- **ELECTRONIC DENSITY OF STATES**
- **MAGNETIZATION**
- **SUPERCONDUCDTING TRANSITION TEMPERATURE**
- **STRENGTH, STIFFNESS, DUCTILITY**

A very significant breakthrough in superconducting materials has occurred recently which may have a major effect on high density integrated circuits. A new class of superconducting materials [3] whose zero resistance transition temperature has been measured to be as high as 93K has been reported.[4] This temperature is well above that of liquid nitrogen which is an economical refrigerant. The possibility of still yet higher transition temperatures in related materials is likely. Potential applications of this material to nanometric ultra high density circuits include interconnects between active devices as well as the possibility of new types of active devices. A zero resistance interconnect superconducting line exhibits no thermal dissipation and zero dispersion. The former condition reduces total heat generated per unit volume and relaxes the need for high gain devices while the latter condition reduces the propagation time of signals between active devices. To be technologically useful for electronic applications, these new high Tc materials will have to be deposited in high quality crack-free thin films and have critical current densities in excess of about 10^3 amperes per centimeter squared. At the present time the scientific understanding of these materials is increasing at an astounding rate. It is impossible at this time to predict the total impact these materials will have on the future of ultra-high density integrated circuits.

Processing Science

Pattern definition (lithography), pattern transfer (etching), and low temperature processes require substantial research to extend present technology to the nanometer regime. Planar processes must be developed that achieve reproducible results in nanometric dimensions over large areas without creating yield-inhibiting defects. Advances in lithography, etching, and low temperature deposition processes are necessary.

The three performance parameters of significance for lithography are resolution, registration, and throughput. Energy sources used to expose or otherwise produce the pattern may be photons, electrons, or ions. The three lithographic techniques for performing the exposure are proximity or contact printing, projection printing, and focused beam direct writing. In the near term, optical lithography for ultra large scale integration (ULSI) may be extended to 0.25 micrometer design rules by direct step on wafer projection aligners now in development. These steppers use short UV optical columns and excimer laser sources. For feature sizes much less then 0.25 micrometers, optical lithography becomes resolution limited because of diffraction. X-ray lithography by proximity printing is the approach most likely to become the high through-put manufacturing lithographic tool for patterning features less than 0.25 micrometers to about 10 nanometers in dimension. Radiation for such exposure tools may come from synchrotron storage rings, plasma sources (e.g. laser heated plasma sources), or traditional electron-impact vacuum sources. Electron beam lithography is important for both present and future lithographic processes. Well developed e-beam tools are used for producing masks for other lithographic manufacturing processes as well as a direct write-on-resist tool for producing structures with nanometer dimensions for research purposes. For both electron beam and x-ray exposure, radiation sensitive polymer resists are used. The chemical changes in the resist, necessary for pattern definition, are produced by the slow secondary electrons produced in the irradiation process. These electrons form a scattering and straggling cloud which sets the ultimate resolution limits for these forms of lithography. Ions are also used as a source of radiation for lithography both as focussed-ion and masked-ion beam technologies. However, radiation damage in the substrate appears to set a significant limitation to this approach for achieving nanometer geometries since focussing and exposure requires high ion energies. Figure 3 summarizes the various approaches to lithography as a function of design rules and projects limits of these approaches for the nanometer regime.

Figure 3

Approaches to lithography, mask making, and replication.

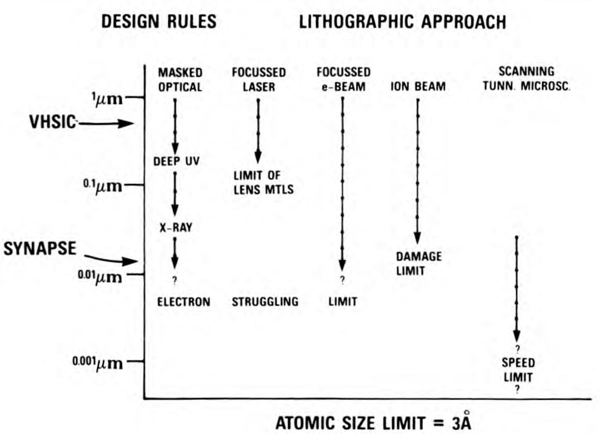

All these lithographic methods require advances in resist technology. Such developments are not trivial because higher resolution patterning requires thinner resist films which are sufficiently robust to withstand pattern transfer mechanisms. New resist materials based upon polysiloxanes are being developed as possible e-beam resists, and organic monolayers deposited by Langmuir-Blodgett techniques also are being investigated. There are, however, several approaches to patterning which are not dependent upon the exposure of resists. In one such approach being investigated at the Naval Research Laboratory, incident electrons produce core-holes in physisorbed molecules like nitrogen on silicon. Using the Knoteck-Feibleman process, it may be possible to produce a monolayer of silicon nitride in the local region exposed to the electron beam. Another approach with some promise for patterning in the nano-regime is based upon the scanning tunneling microscope (STM). Surface resolution at the atomic scale has already been demonstrated by existing instruments. Lithography may be possible by inelastic tunnelling process on surfaces using the STM probe, depositing conducting materials resistant to subsequent etching processes, or exposing organic, inorganic, or halide resist systems.[5] In all cases which use focussed or point beams to perform pattern definition, two significant factors are the time necessary to write the complete pattern and the accuracy of the shapes produced when correlated with the original data set design. Thus, writing speed and noise in the computer driven beam control system will be the practical factors determining the applicability of these tools to manufacturing.

Pattern transfer of small features is accomplished in present processes almost entirely by dry etching as opposed to wet etching. Table 3 lists the qualities of these two approaches. An approach to dry etching which has promise for extension to pattern transfer in the nanometric regime is chemically assisted ion beam etching. This process uses inert ions, such as argon, which bombard the surface to be etched and stimulate highly selective etching by chemically active gases. Figure 4 shows the increase of etch rate in the presence of an ion beam as opposed to that rate in which either ions or chemically active gases are used by themselves.[6] Much is not understood about this process. Research based upon in-situ optical probes and Raman spectroscopy is being brought to bear on the problem to identify the mechanisms which are occurring within one or two monolayers of the surface. This understanding will lead to advances in the technological significance of this form of dry etching. Direct pattern transfer by focused ion beam writing is also possible if substrate damage could be made negligible.

Other process related issues that need attention to extend current technology to the nanometer regime are: control of dimensional non-uniformity; control of the structure of interfacial regions; and reliability of small devices specifically in the areas of electromigration, process induced damage, and single event upsets. In particular, the degradation of carrier mobility due to surface and interface scattering, film stress, and charge trapping will be an important performance issue in new device structures. These effects are predicted to disappear with the advent of atomically perfect interfaces and surfaces produced by low temperature MBE or MOCVD. Fluctuations in dimensional uniformity will also be a major issue in nanometric devices.

Table 3

A comparison of wet and dry processes for pattern transfer.

WET ETCHING
- **CRYSTAL ORIENTATION DEPENDENCE**
- **SELECTIVITY GOOD, DEPTH CONTROL POOR**
- **SIDEWALL CONTROL LIMITED**

DRY ETCHING
- **GOOD SELECTIVITY**
- **GOOD ANISOTROPY, SIDEWALL CONTROL**
- **GOOD DEPTH CONTROL**
- **POTENTIAL FOR MASKLESS ETCHING WITH FOCUSSED IONS**

Figure 4

Synergy of chemical and ion bombardment effects for anisotropic dry etching (ref. 6).

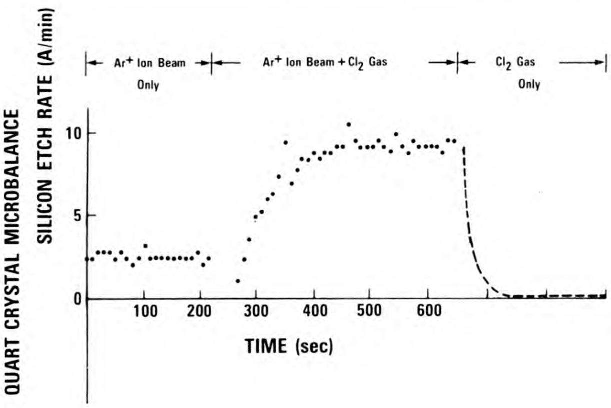

Figure 5

Schematic cross-section of a single well double-barrier resonant tunneling structure and its corresponding I-V characteristic. (ref. 9)

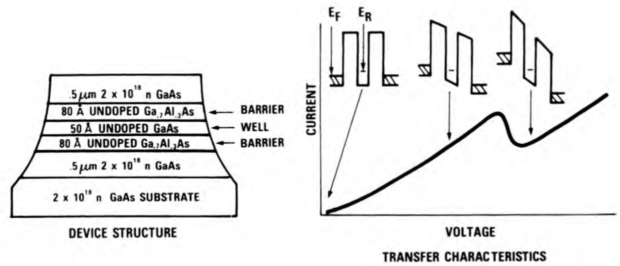

Device Physics

The important properties of new devices for future nanometer circuits are charge transport, noise, and very low heat dissipation. The ability to form artificially structured materials by MBE and MOCVD produce unique scientific opportunities for the study of charge transport phenomena in layered microstructures as well as the exploitation of these effects for new devices. Doping superlattices, compositional superlattices, and quantum well structures have been produced in semiconductors and metals. The most extensively studied material system is that of GaAs/AlGaAs. This is due in large part to the direct bandgap of GaAs and its alloys, and the ability to form lattice matched layers over a wide range of stoichiometry. For example, scientific studies have included measuring the effects of confinement on shallow donor binding energy in quantum wells,[7] changes in the effective bandgap of doping superlattices and modulation of the bandgap of compositional superlattices by strain are but a few. The first technologically significant exploitation of artificially structured materials has been modulation doping.[8] In its rudimentary form, a two dimensional electron gas is formed at the interface between a highly n^+ doped AlGaAs layer and an intrinsic layer of GaAs. Because the conduction band of the AlGaAs is higher in energy than is GaAs, donor electrons from the AlGaAs are confined to the GaAs side of the interface in which there are few donor impurity scattering centers to impede mobility. This modulation doping mechanism for enhancing electron mobility above that which is normally found in the active device channel has been exploited technologically to make a new type of field effect transistor called the MODFET which exhibits high switching speed and high transconductance.

Another phenomenon which is characterized by inherently high speed is that of charge transport by quantum mechanical tunneling. This mechanism is one which may be used for switching between novel devices in nanometer circuits of the future. Figure 5 shows the cross section of a single well double barrier resonant tunneling structure and a corresponding I-V curve for such a device showing negative differential resistance attributed to tunneling of electrons through the quantum well.[9] Resonant tunneling occurs when bias conditions place the quantized electron sub-band in the GaAs well opposite the Fermi energy for carriers in the GaAs region beyond the AlGaAs barrier. As increasing bias voltage moves the sub-band below the energy of the electrons, in the GaAs contact region, the current decreases. The charge transport through the barrier can be faster then 0.1 picoseconds. Another type of resonant tunneling device is the quantum state transfer device[10] illustrated in Figure 6. A photomicrograph of this device is shown on the cover of this issue. In this device a high mobility GaAs channel is separated from a lower mobility AlGaAs channel by a thin (<100A) barrier of AlGaAs formed with high Al content. The electrons are in quantized sub-bands at zero bias potential across the device. As their energy increases under an applied electric field, tunneling through the barrier into the lower mobility channel occurs when the sub-band energies coincide, producing negative differential resistance. As in the resonant tunneling device, charge transport through the thin barrier region is extraordinarily fast. Finally, another new class of high speed device structure is based upon Aharonov-Bohm quantum interference of electrons.

Figure 6

I-V characteristics of a quantum state transfer device showing negative differential resistance. (ref. 10)

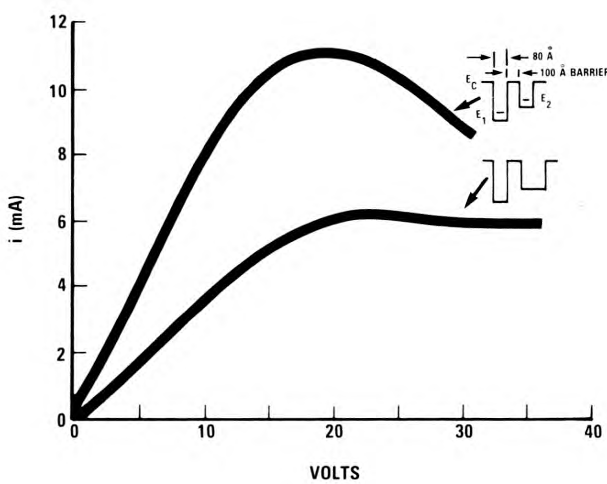

Figure 7

Novel three terminal solid state switch which utilizes the superconducting proximity effect.

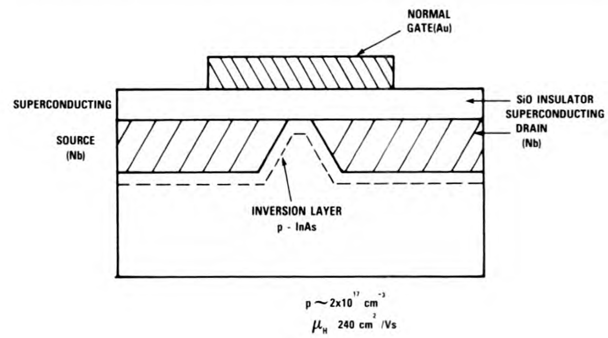

A suitably small conducting channel is separated into two parallel contiguous conducting channels. A controlled phase shift is applied to one arm of the device by either an applied electric or magnetic field. Recombination of the two arms produce an interferometric effect which modulates the current through the device. Devices based upon this effect offer interesting possibilities of extraordinarily low power dissipation and picosecond switching.[11] They inherently require nanometer feature sizes to produce quantum wavefunction phase coherence. Aharonov-Bohm interference oscillations have been observed experimentally in GaAs heterostrucutres[12] as well as certain metallic structures. Other novel approaches to active devices rely upon conducting channels created by the superconducting proximity effect[13] as shown in Figure 7. The device is a semiconductor-coupled Josephson junction in which the insulated gate serves to modulate the channel inversion layer between the two Nb superconductors. The discovery of new high temperature superconductor materials promises to revitalize research into novel superconductor devices.

In the more distant future, devices which consist of structures only a few nanometers thick will exhibit one-dimensional effects. In these structures electrons cannot get past each other except by hopping. Localization effects may further hamper transport.

Noise will be a fundamental limiting factor in nanometric devices. Operating voltages of nanometric circuits are likely to be substantially lower than present 3 and 5 volt values to maintain reliability and lower power dissipation. Therefore, noise margins will be reduced. Thermal noise can be reduced by cooling if necessary. However, shot noise will increase in significance at reduced voltages. One possibility is to suppress shot noise using Coulomb interactions in charge transport analogous to the extremely strong depression of shot noise by space charge in vacuum electronic devices.[14] In nanometric devices these interactions may make it possible to create electron-electron correlation for emission over or tunneling through a barrier. The effect of dimensional non-uniformities is also likely to manifest itself as fluctuation noise in nanometer structures. A sound understanding of these effects, based upon new ideas in statistical mechanics, will be necessary.

Nanometric monolithic circuits will require devices with very low heat dissipation to maintain operating temperatures within the device which do not cause reliability and performance degradation. The ability to maintain a prescribed temperature is to first order dependent upon the thermal conductivity of the semiconductor substrate material. Of the common semiconductor materials, silicon has the best thermal conductivity at room temperature (1.5 W/cm-K). GaAs has a thermal conductivity at room temperature of 0.46 W/cm-K while diamond is over an order of magnitude better at 21 W/cm-K. At low temperatures (15-100 K) thermal conductivity of all these materials improves and the performance gap between diamond, silicon, and GaAs closes. Technological approaches to facilitate heat removal may also be applicable such as the incorporation of passive micro-channel heat pipes in the chip substrate.

The sources of power dissipation within the circuit arise from the finite resistance of the active device, the dynamic power dissipation caused by the rate of switching, and the resistance of the interconnections between active devices. The first factor will require novel device structures which may be based upon principles of operation described earlier. Reduction in dynamic power dissipation requires minimization of parasitic and interconnect capacitances. Although not a factor in present integrated circuits, the finite resistance of interconnections on the nano-scale could make a significant contributor to dissipation. The recent scientific breakthroughs in high temperature superconductor materials may obviate this issue.

Circuit Architectures

Present circuit architectures for computers and artificial intelligence machines for the most part use the von Neumann approach of linear programming applied sequentially to bit-conserving electronic logic circuits (Thinking Machine Inc.'s Connection Machine computer is a notable exception). This approach has led to vast improvements in computers centered upon the hardware development of the CPU/microprocessor and large core/DRAM memories. However, a major performance limiter for monolithic circuits is signal propagation time between gates. Present circuit architectures and their corresponding physical implementation do not inherently minimize the interconnection lengths between functional logic elements. Consequently, the signal propagation time due to the interconnection and not the device switching speed is the performance limiting element in these circuits. This situation would be exacerbated in the nanometric regime in which the inherent switching speeds will be one to two orders of magnitude faster. New approaches to computing algorithms and architectures are necessary. One such new class of algorithms for adaptive information processing is based upon analogies of the functional neural elements of the human brain and has motivated a growing number of new investigations into circuit architectures and implementations. Table 4 compares some of the trade-offs between present computer architectures and those of the human brain. These differences suggest that present architectural approaches are not well suited to the implementation of electronic neural networks. Their functional ability is based upon large scale connectivity of primitive logic elements while in present machines this form of connectivity is limited. The human brain may have as many as 10^{11} neurons each with a hundred to ten thousand synaptic input connections. There are then about 10^{14} synapses. The response of these synapses are binary although their inputs are analog in nature. Also there are reciprocal reentrant connections. This highly parallel connectivity and multi-functionalism is responsible for the brain's inherent immunity to single point failure. Hopfield has demonstrated an associative memory neural network algorithm which can be implemented in a specific circuit and is applicable to a large generic class of pattern recognition problems.[15] As a result, much interest has been focused upon neural network research and progress has been made in creating new algorithms to simulate them. In some cases the corresponding silicon microelectronic monolithic circuits have been implemented.[16] The full realization of neural network computational circuits will best be realized by large arrays of multiply interconnected devices. These arrays must have the attribute of minimum interconnection lengths between functional elements. Such array architectures may be possible in the nanometeric regime. The inherent tolerance of neural network functionality to isolated single point failures may also be a crucial attribute which significantly impacts manufacturing yield of future nanometer technologies.

Table 4

Some comparisons between human brain function and present day computers.

HUMAN BRAIN	COMPARED TO	COMPUTER/ AI MACHINE
POOR AT ARITHMETIC		POWERFUL AT ARITHMETIC
GOOD AT PATTERN RECOGNITION		POOR AT PATTERN RECOGNITION
CONTENT - ADDRESSABLE MEMORIES (SIMILARITY ADDRESSABLE)		RANDOM ACCESS MEMORIES (LOCATION ADDRESSABLE)
ROBUST AGAINST DEVICE FAILURE		SENSITIVE TO DEVICE FAILURE (ERROR CORRECTION CODES)
COLLECTIVE FUNCTION		NON - COLLECTIVE FUNCTION
FAST OPTIMIZATION PROCEDURES		SLOW OPTIMIZATION PROCEDURES
PLASTIC SYNAPSES		REPRODUCIBLE DEVICE ACTION

Conclusion

The scientific foundation for a next generation of revolutionary solid state electronic technologies is being built in laboratories throughout the world. This research will continue to drive the revolution in information, computer, and electronics technologies producing new, faster, smaller, and more powerful electronic systems. These future device and circuit technologies will be based upon structures with dimensions in the nanometric regime and in which quantum effects will play an important role. As the limitations in conventional process technology and device physics of traditional silicon microelectronics are reached over the next seven to ten years, improvements in chip performance and device density will become incremental. Alternate approaches for continued progress such as low temperature operation, wafer scale integration, novel packaging and thermal management, advanced concepts in chip architecture which improve speed performance by better management of signal carrying interchip interconnections, and improvements in chip yield will then resist the transition to the nano-regime. The scientific and technological challenges are in themselves extraordinary. However, the basic outline of what needs to be accomplished is known and research opportunities are abundant. If the revolution caused by the silicon integrated circuit in our everyday life is an example of what can be achieved then the benefit to the realization of nanometer scale electronics will be enormous. Human intellect, ingenuity, and curiosity will surely strive to open these new frontiers.

Acknowledgments

The cumulative contributions of the senior staff of the Electronics Technology Division, Naval Research Laboratory is acknowledged. In particular, the contributions and discussions held with R.F. Greene and S.G. Bishop have been particularly helpful. Much of the contents of this paper were first presented at the Molecular Electronics III Conference held in Crystal City, Virginia in October, 1986, and subsequently published in the Conference Proceedings.

Biography

G.M. Borsuk is the Superintendent of the Electronics Technology Division, Naval Research Laboratory, Washington, D.C. He has conducted research and published articles on solid state photodetectors and novel microelectronic devices.

References

1. Semiconductor Research Corp. Newsletter, Vol. 4, No. 8, p. 1, Aug. 1986.

2. A.C. Warren, D.A. Antondiadis, H.I. Smith, and J. Melngalis, IEEE Elec. Dev. Let., Vol. EDL-6, No. 6, p. 294, June 1985.

3. J.G. Bednorz and K.A. Muller, Z. Phys., B 64, p. 189, Sept. 1986.

4. M.K. Wu, et al., Phys. Rev. Lets., Vol. 58, No. 9, p. 908, March 1987.

5. P.K. Hansma and G. Tersoff, J. Appl. Phys., Vol. 61, No. 12, p. R18, Jan. 1987.

6. J.W. Coburn and H.F. Winters, J. Appl. Phys., Vol. 50, p. 3189, 1979.

7. R.V. Shanabrook, Surface Science, Vol. 170, p. 449, 1986.

8. R. Dingle, H.L. Stromer, A.G. Gossard, and W. Wiegmann, Appl. Phys. Lett., Vol. 33, 7, 1 Oct. 1978.

9. T.C.L.G. Sollner, W.D. Goodhue, P.E. Tannenwald, C.D. Parker, and D.D. Peck, Appl. Phys. Lett., Vol. 43, No. 6, p. 588, Sept. 1983.

10. S.W. Kirchoefer, R. Magno, and J. Comas, Appl. Phys. Lett., Vol. 44, No. 11, p. 1054, June 1984.

11. S. Bandyopadhyay, et al., Proc. of the 1986 IEDM, Sec. 4.1, p. 76, Dec. 1986.

12. S. Datta, et al., Phys. Rev. Lett., Vol. 55, p. 2344, 1985.

13. H. Takayangi and T. Kawakami, Proc. 1985 IEDM, p. 98, 1985.

14. R.F. Greene, private communication.

15. J.J. Hopefield, Proc. Natl. Acad. Sci., Vol. 81, p. 3088, 1984.

16. J.J. Hopefield and D.W. Tank, Science, Vol. 233, p. 625, 1986.

Acoustic Images of Target Range in the Sonar of Bats

By James A. Simmons
Brown University

Photograph of the big brown bat, Eptesicus fuscus, *showing the external ears, which act as receiving antennas for the bat's sonar system. The horn shaped* pinna *is the echo gathering element, and the blade-shaped* tragus *is a secondary reflector that generates cues for determining the elevation of a target. The horizontal ridges on the pinna facilitate reflections towards the tragus for a wide range of target elevations. The sound spectrogram of an echolocation signal is shown below. This species emits its sonar sounds through the mouth.*

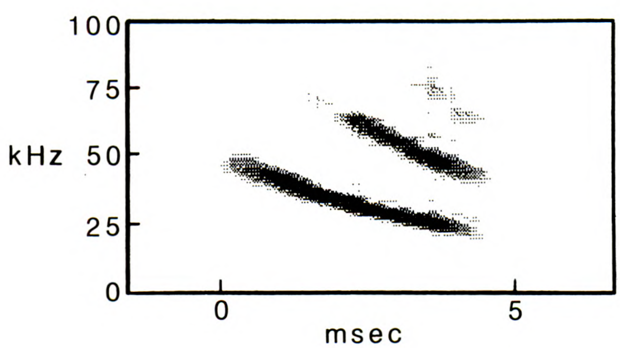

This article describes work that ONR has been supporting because of its interest in theories of information processing that have a possible application to the problem of classifying transient and active acoustic signals. The ability of bats to perceive the environment with a biological form of active sonar called echolocation[1] provides a scientific opportunity to study echo signal-processing and real-time extraction and display of information about targets in echoes, and execution of decisions involving target localization and classification, that exceeds present technological capabilities. There are indications that the bat's brain, acting as the sonar receiver, mixes the functions of signal reception, signal processing, target display, and control of spatially-oriented actions in a nested fashion that incorporates both parallel and hierarchical processing of information.[2]

It would be useful to know whether the bat employs novel techniques either to represent and process echoes or to display images of targets. This article describes the content of the images that echolocating bats perceive along the psychological dimension of target range. Knowledge of constraints imposed by the physiological properties of the bat's auditory representation of sonar echoes (the biological analog-to-digital code the bat uses) leads to a unique interpretation of these images and helps us to understand the nature of the bat's sonar receiver.

Echolocation and Perception of Target Range

Bats are mammals, belonging to the order Chiroptera, whose lives are almost entirely nocturnal.[3] They have evolved powered flight for locomotion and echolocation for orientation in darkness, and with this combination they achieve an unparalleled freedom of movement and action at night. Echolocation is a naturally-occuring adaptation of the vocal and auditory systems that joins their capabilities to create a sonar system. The bat's larynx and vocal tract act as the transmitter, while the ears and auditory system act as the receiver.[1,4,5] An echolocating bat emits a series of brief, mostly ultrasonic sounds and perceives objects in its immediate environment from the echoes of these sounds that return to its ears. By reflecting sounds off objects, the bat in effect induces them to reveal their presence, location, and character as though the objects themselves were the source of the sounds. The practice of echolocation requires an unusual degree of coordination of sound production and hearing, which makes it similar in some respects to human speech. Whereas speech sounds lead eventually to representation and then perception of the objects and ideas conveyed in words and sentences, the bat's sonar sounds lead to representation and then perception of the spatial location and appearance of objects. Not surprisingly, the bat's auditory system is specialized for extracting and representing the spatial information about sonar targets that is conveyed to the bat by the acoustic features of echoes.[2,6,7] These representations lead to perception of images of targets by the bat that are expressed in spatial coordinates or are so readily transposed into spatial terms that they routinely can guide the bat's flight.

Interception of Flying Insects by Sonar

There are over 700 species of echolocating bats, the majority of which are insectivorous and make their living by feeding upon insects that are captured in flight after having been located by sonar. Bats capture flying insects in a stereotyped interception maneuver that is similar, and thus amenable to comparison, across most species. Although bats use their sonar to perceive all sorts of objects in their immediate vicinity—to navigate and detect obstacles to flight, for example—the use for which echolocation is most closely adapted is the detection, tracking, and identification of prey. As evidence for this close coupling of echolocation to pursuit of flying insects, the structure and the pattern of emission of sonar sounds are correlated in different species with differences in the acoustic strategies they use for finding prey and with conditions prevailing from moment to moment in each individual pursuit maneuver.[5,8,9,10] Furthermore, the representation of echo and target features in the bat's brain closely follows the structure of the bat's sonar sounds in the context of the interception maneuver.[2,6] The images that the bat actually perceives of targets depend upon the structure of the sonar sounds and the requirements of finding prey.[11,12,13,14] It thus seems that the quintessential behavior for which bats use their sonar is the pursuit of flying insects.

Figure 1 shows a diagram of the process of interception of a flying insect, based upon stroboscopic photographs and tape recordings of numerous pursuits by the little brown bat, *Myotis lucifugus,* and the big brown bat, *Eptesicus fuscus,*[1,15,16] by the pipistrelle bat, *Pipistrellus kuhli,*[17] by the horseshoe bat, *Rhinolophus ferrumequinum,*[18] by the mustache bat, *Pteronotus parnellii,*[19,20] and by two other species of *Pteronotus.*[21,22] These species represent nearly all of the different types of echolocation systems found among bats, and photographic studies establish that the interception maneuver appears substantially the same in all of them. The process of interception shows several stages that are associated with the pattern of emission of sonar sounds and other aspects of the bat's behavior with respect to the target. For example, the bat regulates the rate of emission of its sonar sounds according to the progressively-declining distance to the target (see "sound track" in Figure 1) and follows the target's location by keeping its head pointed at the target as it approaches. Photographs indicate a head-

Figure 1

Diagram of an interception maneuver by an echolocating bat.[36] *The bat and the insect are each shown as numbered images based on stroboscopic photographs taken at intervals of 100 msec. A thin dotted line connects corresponding images of the bat and the target to show target range. The flight path of the bat provides a "sound track" of sonar signals, with the occurrence of each emission indicated by a short bar perpendicular to the flight path at the location of the bat when it produced the sound.*

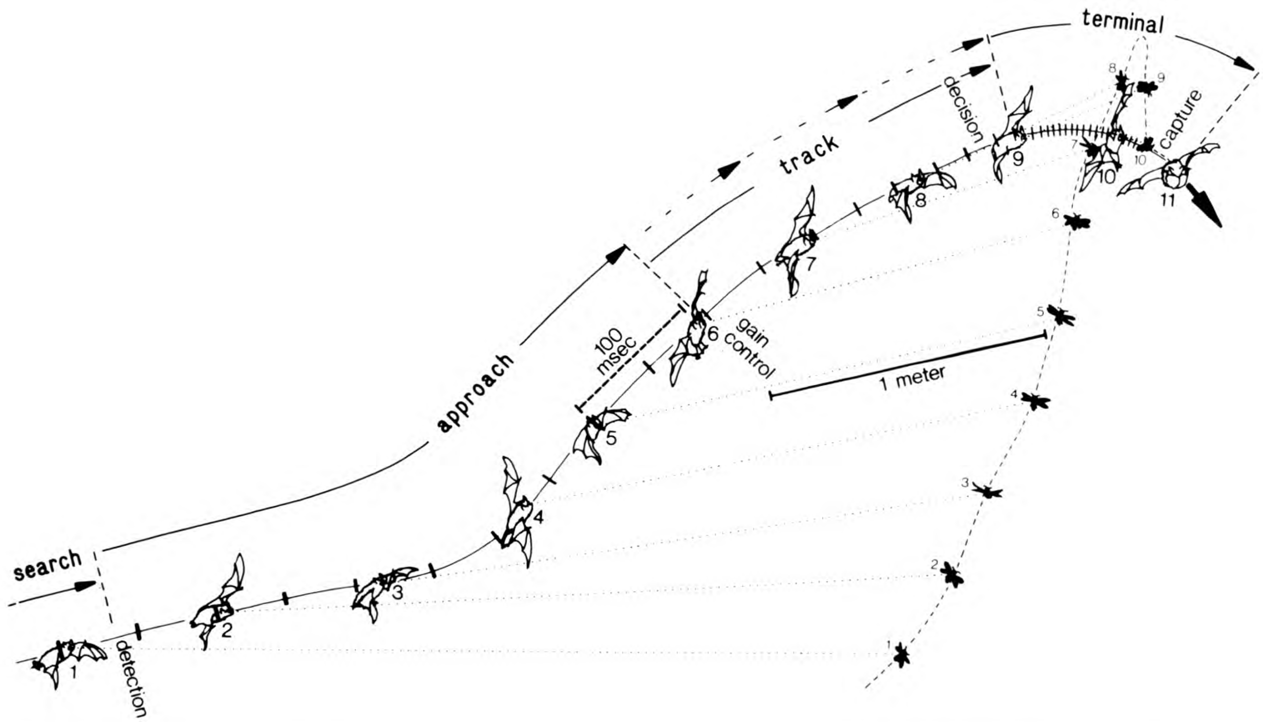

aim tracking accuracy of at least 5°, and experiments under controlled conditions reveal that the bat's tracking system probably is accurate to within 1 to 2°, which corresponds to the sharpness of target images in the horizontal plane.[23,24] These various tracking responses confirm that the bat is aware of the target's location in three dimensions throughout the interception maneuver.

The images that the bat perceives of the target throughout the pursuit maneuver naturally depend upon the characteristics of the sonar signals; these in turn produce the echoes which give rise to the images. Figure 2 shows the composition of the individual sonar sounds in a series of signals emitted by the big brown bat, *Eptesicus fuscus*, as it intercepts a flying insect.[5] The sounds are illustrated in terms of their time-frequency structure, or spectrograms. A spectrogram representation is useful because it visually conveys more information about the signals than other kinds of illustrations such as their time waveforms or their overall spectra. This spectrogram record of pursuit shows 34 numbered sounds that extend over a period of about one-and-a-half seconds leading up to the capture of the insect. Each sound yields a discrete image of the target, and the pursuit maneuver is guided by what must amount to a kind of acoustically-derived motion-picture of the insect in relation to the attacking bat. The most notable features of these sounds are that they are frequency-modulated (FM), sweeping downward in frequency from beginning to end; they are quite brief, each lasting only a few milliseconds; and they contain relatively high sound frequencies, typically above 20 kHz.

The first three sounds in Figure 2 sweep shallowly in frequency from about 28 to 22 kHz in the first harmonic and from 56 to 44 kHz in the second harmonic. These are signals used to search for targets; when the bat begins reacting to the target's presence, the FM sweeps abruptly change from shallow to steep (compare sound No. 3 with sound No. 4 in Figure 2). After the target has been detected and pursuit is joined, the bandwidth of the sounds broadens considerably. Now, the first harmonic sweeps from 50-60 kHz down to about 25 kHz, with the second harmonic sweeping from about 100 kHz down to 50 kHz. (Frequencies above 75 kHz do not appear in Figure 2; their

Figure 2

A continuous spectrogram record of a sequence of echolocation sounds emitted by Eptesicus fuscus during a pursuit maneuver.

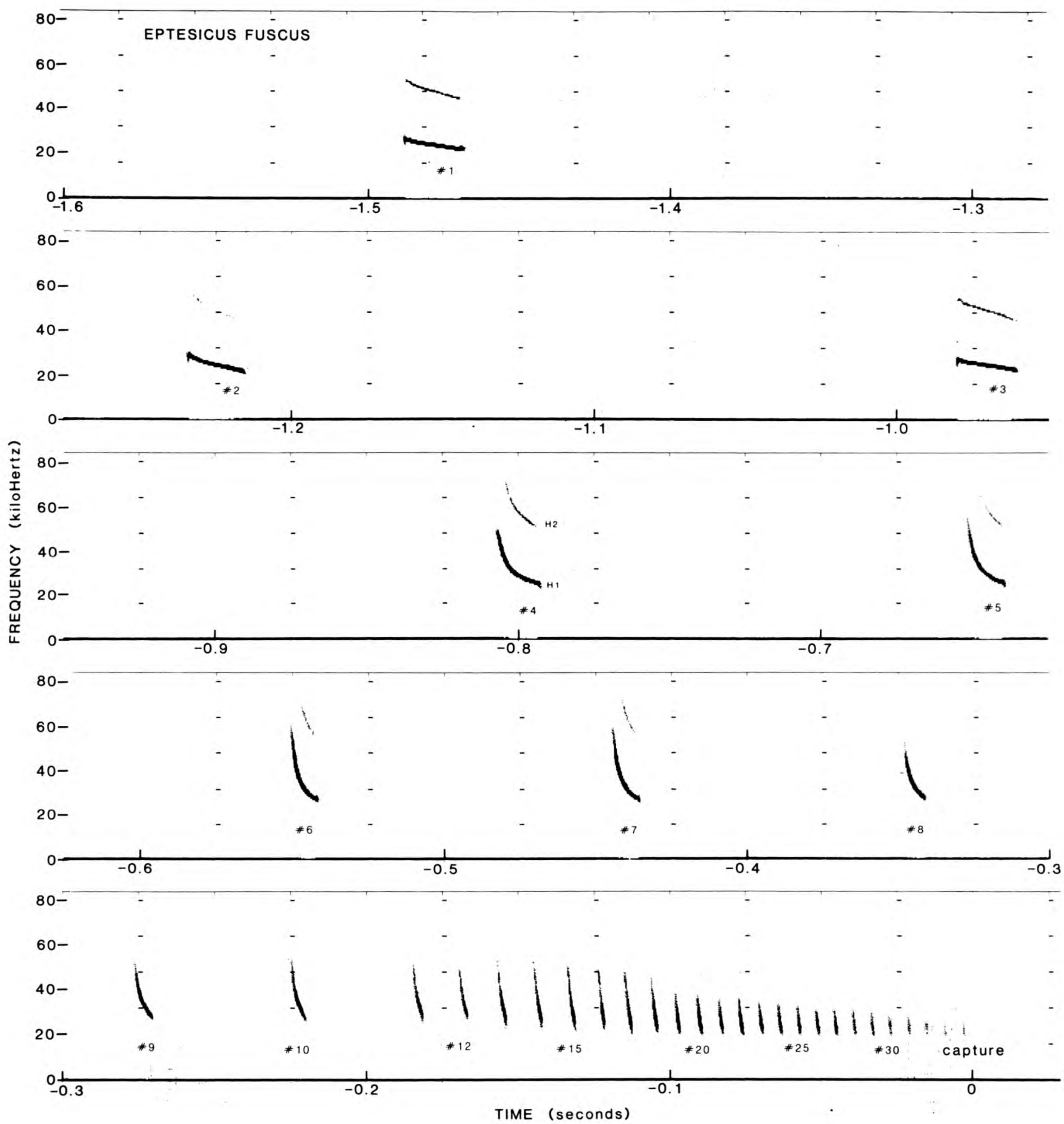

absence is an artifact of sound absorption by the atmosphere at high ultrasonic frequencies.[25] Higher frequencies are present in recordings made with the bat closer to the microphone, however.) These broad FM sweeps provide a range of frequencies with which to form sharp, information-rich images of the target.[13] The bat's acoustic behavior during active pursuit documents its interest in the target—showing, for example, that the bat tracks the target's declining range.

The pursuit maneuver culminates in a brief burst of rapidly-accelerating sonar emissions (beginning with sound No. 11 in Figure 2) and the actual capture of the target (see Figure 1). The bat reaches out at the last moment to seize the insect in its wing or tail membrane.[26] The use of the flight membranes to gather in the target provides a valuable indication of the accuracy with which the bat has determined the target's location by the end of the maneuver. From multiple-flash photographs of interceptions, the bat appears to know the target's position in three dimensions to within about 1 to 2 cm at the moment of capture. By dusting insects with flour before the bat is given the opportunity to capture them and then measuring the extent of wing surface whitened from contact with targets, the accuracy of the bat's reach has been confirmed at 1 to 2 cm.[27] Photographs such as Figure 3 show the bat's wing-tip curled around the target in evident anticipation of capture, revealing that target range is known and used explicitly to guide this movement. The results of all these observations suggest that a mechanical accuracy of reaching to within 1 to 2 cm of the target's true position is sufficient to result in successful interceptions; no greater accuracy is manifested in this aspect of the bat's behavior.

Figure 3

A stroboscopic photograph of a little brown bat, Myotis lucifugus, reaching out to seize an airborne mealworm with the tip of its left wing at the culmination of a pursuit.[15] The target is outlined to make it visible against the highlight reflecting from the bat's wing. Notice the shadow of the target on the wing-tip. (Photo courtesy of F.S. Webster.)

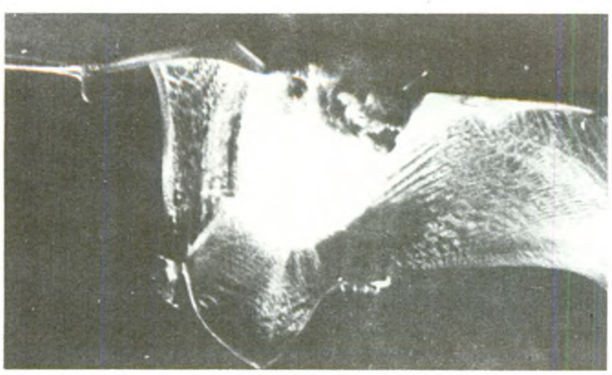

The Operating Range of Echolocation

Since the primary use for echolocation is the detection, tracking, identification, and interception of flying insects, we can take the distances over which bats encounter and actively pursue prey to be the operating range of echolocation, at least for most practical purposes. Species of bats differ in the distances at which they first react to flying insects, but these distances seldom seem to be greater than a few meters.[8] The largely ultrasonic sonar transmissions of bats occur at frequencies where the atmosphere is not an ideal medium for propagation. An appreciable fraction of the energy in echolocation sounds is absorbed by the air as the sound travels to and from the target.[25,28,29] Furthermore, only a small fraction of the energy in the sound that strikes an insect-sized target is reflected or scattered back in the direction of the bat.[29,30] Consequently, the echoes reaching the bat's ears are relatively weak under most circumstances. Aerial-feeding insectivorous bats typically transmit very intense sounds for echolocation—sound pressures of 100 to 110 dB SPL (peak-to-peak) are common. Nevertheless, bats must be fairly close to small targets to receive echoes that are audible to them. For this reason echolocation is a relatively short-range mode of perception, although one must remember that it still permits the bat to find flying insects in the dark, when they cannot be seen.

The distance at which bats can first detect small targets, and thus begin to actively pursue them, has been estimated from observation of interceptions and measured directly in psychophysical tests. In laboratory experiments the big brown bat, *Eptesicus fuscus,* can perceive a sphere with a diameter of 5 mm as far away as 3 meters, and it can perceive a 20 mm sphere as far away as 5 meters.[31] The sonar echoes reaching the bat's ears from such small spheres at the maximum distances of detection have amplitudes approximately at the bat's threshold of hearing.[32] When bats are actually pursuing prey, they might not perform as well as they do in laboratory tests under quiet conditions, but observations of interceptions have shown that they certainly react to small insects and to targets such as 3- to 10-mm spheres at distances of about a meter.[1,15,17] *Eptesicus fuscus* will react to individual mealworms thrown into the air when the target is as far away as 2 meters.[16] Field observations reveal comparable distances of reaction to natural prey by other species of bats.[8]

The records of sonar sounds emitted by echolocating bats during actual pursuit maneuvers (Figure 2) provide two sorts of estimates of the probable distance of detection, and it is instructive to examine how these are obtained.[1,17] *Eptesicus fuscus* is representative of a large category of echolocating bats that emit predominately FM sonar sounds. These bats all keep their individual signals short enough that the emitted sound is finished well before the echo of that sound starts to arrive at the bat's ears.[16,33] When approaching a target, the bat shortens its echolocation sounds in proportion to the decreasing interval between emissions and echoes; or to the target's decreasing distance. The bat first exhibits this progressive reduction in signal duration when the target is detected and it is near enough that the outward and return travel time of each echo is so short as to encroach upon the duration of the sound.[4] As the bat flies closer to the target the signals become shorter and the rate of emission of sounds increases. In Fig. 1, the bat begins to accelerate the emission of sounds following reception of the echo of sound No. 3. This sound has a duration of 18 msec. at a velocity of sound of 344 m/sec, overlap of the echo with the emission would begin to occur when the bat is 3.1 meters from the target.

The entire series of sounds shown in Figure 2 provides a second estimate of the distance at which the bat first reacts to the insect's presence. Bats of the species *Eptesicus fuscus* commonly fly at speeds of about 3.4 m/sec when pursuing insects in a large laboratory room.[16] The bat whose sounds appear in Figure 2 first reacted after receiving the echo of sound No. 3, which occurs about a second prior to the eventual interception. Assuming a more-or-less straight flight-path at a constant velocity for the bat as it approaches the insect, the bat must have been somewhat nearer than 3.4 meters when it received the echo that provoked its response. Both of the estimates of the distance of detection based on the bat's acoustic behavior are in reasonable agreement with the results of psychophysical experiments that show *Eptesicus* to be capable of detecting insect-sized targets at distances of 3 to 5 meters.

The Perceptual Dimension of Target Range

To an echolocating bat the sensation of depth in the immediate environment is provided through its sonar system in terms of a unitary psychological dimension of target range. This psychophysical axis incorporates both the distance to individual targets as an estimate of how far away each is from the bat, and also the differences in distance to different parts of a complex target whose parts are distributed at intervals along the range axis. Bats actually perceive the depth or range "profile" of a target as a means of determining target shape, and these differences are perceived around the absolute distance to the target as a whole. Just how information about these two different kinds of "depth" comes to be extracted from sonar echoes and then expressed together along a single psychological dimension can be seen from a combination of behavioral and physiological observations of echolocation.

Acuity of target ranging: Bats perceive the distance to individual targets from the time-delay of echoes, and they can use time-delay to distinguish among targets located at different distances in terms of magnitudes along a psychological target-range scale.[34] For a velocity of sound in air of 344 m/sec, each centimeter of target range retards the arrival of echoes by about 58 μ sec, or 5.8 msec for each meter. (The total path traveled by the sound is twice the target's range—the distance is crossed once on the outgoing journey and once on the return journey.) Psychophysical experiments establish the complete equivalence of target range and echo delay for bats.[34,35], so distance perception is essentially a matter of estimating the duration of the interval of time that elapses between production of sonar sounds and reception of echoes. As the bat approaches a target such as a flying insect, not only do echoes arrive after shorter and shorter delays, but the echoes increase progressively in amplitude (by about 12 dB for each halving of distance) due to the shorter length of the path traveled to and from the target. Bats adjust the sensitivity of their hearing in a time-dependent manner during the short interval of time following the emission of each sonar sound, becoming more sensitive for longer echo delays.[36] This adjustment compensates for distance-dependent changes in the amplitude of echoes that return from targets at ranges from as little as 17 cm to as much as 1 to 2 meters. It appears that the site of this compensatory mechanism is in the bat's middle ear, so the amplitude of echoes reaching the inner ear to stimulate auditory receptors probably does not change for most of the approach to a target during pursuit. Echo delay is thus isolated from changes in echo amplitude and is the specific acoustic cue for target range. This isolation is crucial for preventing the normally-occurring changes in neural response-latency as sounds increase in amplitude from distorting the perception of target range.[37]

Targets are represented along the bat's perceptual axis of target range as events associated with particular magnitudes of range. The scale of these events—that is, the width of the image of a target along the range axis—can be measured in psychophysical experiments, and the results depend a great deal upon the circumstances of the experiment. Under the best of conditions, one would like to know how accurately the bat can determine target distance from the delay of echoes as an estimate of the sharpness of registration of images along the range dimension. This would provide an indication of how acutely the bat displays target range to *itself*. To obtain such an estimate, the bat and the target must be kept stationary because the distance to the target would shift if the bat or the target moved, disrupting the bat's own measurement of range and, in turn, the experimental measurement of the bat's perceptual acuity.[13] One should appreciate that this requires putting the bat in a fairly artificial situation—after all, the bat and the targets that interest it are usually in flight.

The experimental procedure for measuring the limiting acuity of target ranging depends on the fact that the bat emits its sonar sounds at a higher rate (10 to 30 sounds per second) than it scans its head back and forth to examine targets (one or two cycles of head movement per second). From one sonar emission to the next, the bat's head remains in about the same place; the distance that the bat's head moves only adds up to substantial amounts over a period of time containing perhaps 5 to 10 separate sounds. Consequently, if the bat could be induced to measure a change in the delay of echoes from one sonar emission to the next, that change in echo delay would be relatively uncontaminated by artifacts originating in the bat's own movements. The bat is trained to sit on a small, elevated Y-shaped platform, with its starting position about at the center of the Y, and to broadcast its sonar sounds in the direction of the left and right branches of the Y.[34,38]
A microphone that is sensitive to ultrasonic frequencies is placed at the end of each arm of the Y to pick up the bat's sonar emissions, and each microphone's signal is conducted through an electronic *target simulator* to a loudspeaker placed some distance further away from the bat than the microphone. The electronic apparatus returns echoes to the bat from the loudspeaker after a predetermined delay to mimic the presence of a sonar target at a particular distance. With such a target simulator, one can expose the bat's sonar to test signals that cannot be produced from real objects, and the flexibility of electronic controls permits a direct measurement of the fine acuity of target ranging. In detail, the procedure is to alternate the arrival-time of echoes back and forth from one value to another by changing the electronic delay between one sonar sound and the next. This creates the effect of an artifical target that jumps from one distance to another on succeeding echoes. The jitter is introduced around an average delay of 3 msec, which corresponds to a simulated distance of about 52 cm. The bat is trained with food as reward to detect this jitter in the arrival-time of echoes and to discriminate between the arm of the Y-shaped apparatus that produces jittered echoes and the arm that produces stationary echoes.[35] The presence of jitter in the echoes is shifted from the left to the right from trial to trial in a random fashion. For its response, the bat crawls onto the arm of the platform that is in the direction of the jittered echoes to receive its reward, and the bat's responses to the correct and incorrect arms are totalled for blocks of trials in which a particular jitter value is presented. By reducing the size of the jitter from several hundred microseconds to only a few microseconds in small steps, one can determine the acuity of echo delay perception by the bat.

Figure 4A shows the percentage of errors made by two bats of the species *Eptesicus fuscus* as they discriminated between jittering and stationary targets in the experiment just described. (Data points are solid triangles. In such a two-choice task, perfect performance is zero percent errors, and chance performance is 50 percent errors.) The bats make very few errors for jitters as small as a few microseconds, which corresponds to shifts of only a fraction of a millimeter in target range.

Evidently the bat's sonar receiver can extract information about the arrival-time of echoes and represent it with sufficient accuracy that a change in arrival-time of only about 1 μsec is noticeable to the bat. This is an extraordinary level of acuity for target range of about 0.2 mm, and it is easy to see that the bat's movements during experimental trials, which amount to at least a centimeter along the range axis, would have obscured the limiting accuracy of target ranging if precautions—in the form of the jitter procedure—had not been taken to prevent it.

By plotting the results of the jitter discrimination experiment as the percentage of errors, one can visualize the shape of the image of a target along the range axis. The solid triangles in Figure 4A trace out an approximation to this image. To the bat, a single reflecting source at a fixed distance must appear as a sharply-defined event a fraction of a millimeter wide and centered at the target's apparent range. There are several other features of the image that deserve attention, as well. At distances of about 5 mm and 10mm from the target's true location, the bat exhibits more errors in its performance than at intermediate distances. These "side-peaks" in the image reveal that the bat must sometimes perceive the target to be displaced from its true location to one of these other locations. There is ambiguity in the bat's perception of target range in the sense that several incorrect locations are occasionally confused with the true location. Because the bat has no independent means of knowing the actual location of the target, it sometimes responds to range jitters of 5 or 10 mm as though they were jitter values of zero. The presence of the side-peaks in the bat's performance in the jitter discrimination experiment is important because it reflects structural features of the sonar signals in the image of the target. The reality of these side-peaks was tested through additional experiments in which the echoes being jittered were reduced in amplitude and mixed with broadband noise to tax the bat's sonar receiver more severely. The open triangles in Figure 4A show the performance of one bat detecting echo jitter with the echoes at amplitudes in the vicinity of the bat's echo-detection threshold. This threshold is described as 0 dB sensation level (SL), and the curves in Figure 4A show that the side-peak in the bat's performance at 5 mm becomes more prominent as echoes decline in amplitude relative to threshold. The peculiar two-peaked shape of the bat's performance for jitters between zero and 5 mm is enhanced when echoes are barely detectable.

The acoustic cue that the bat uses to determine target range is the arrival-time of echoes. The bat hears the outgoing sound to mark the start of this time-interval, and reception of the echo marks its termination. During jitter discrimination trials the bat emits a number of sonar sounds at each target, so the image represented by the data in Figure 4A probably is obtained by integrating information across multiple emission-echo pairs. In this respect, too, the data from the jitter discrimination experiment are not realistic; normally the bat would have to judge a target's momentary range from a single emission-echo pair because the target would have moved a great deal by the time the next emission-echo pair occurs. This is all right, of course—the intention of the jitter discrimination experiment was to measure the limiting accuracy of target ranging inherent in the bat's sonar system, not the accuracy that is likely to prevail under natural conditions.

For target ranging, the bat must specify the length of a time-interval bounded by the emission and the echo, and the accuracy of this measurement depends upon the structure of the signals that serve to delineate the interval itself. It is possible to extract from the waveforms of sonar emissions and echoes a representation of all the information contained in these sounds that is relevant to specifying the length of the interval. This representation is the *crosscorrelation function* between emissions and echoes, and the shape of this function is related to the likelihood that the echo will be assigned to a particular value of delay.[39] Figure 4A shows the crosscorrelation function (solid curve) for a typical emission-echo pair, recorded during a jitter discrimination trial, for comparison with the performance of the bats. The graph indicates that the bat perceives the distance to a target or the delay of echoes with an accuracy that corresponds to the half-wave-rectified crosscorrelation function between emissions and echoes. The bat's sonar receiver must somehow extract a representation of echo delay that is equivalent to this crosscorrelation function and then display this representation to itself, if you will, so as to perceive the range of the target.

Under natural conditions the bat would never encounter a target that moves back and forth in place along the range axis from one sonar emission to the next. The bat and the target usually are in flight, making both the form of the simulated jittering target and the circumstances in which the bat observes and responds to the target highly artificial. The combined motion of the bat and the target introduces movement of the target along the range axis by perhaps 10 to 30 cm from one emission to the next. Such large shifts in range produce changes of many hundreds of microseconds in delay on successive echoes, which would completely obscure the existence of a perceptual accuracy of only a microsecond or two in the images that the bat perceives if the target remains stationary. Bats thus are unlikely to perceive the distance to individual sonar targets during pursuit as accurately as during jitter discrimination experiments because the target's normal motion would prevent the integration of information across multiple emission-echo pairs that leads to detection of the jitter.

Figure 4B shows the mean percentage of errors made by 8 bats of the species *Eptesicus fuscus* as they discriminated differences in the distance to two targets—the farther at a distance of 30 cm and the nearer at distances starting at 25 cm and moving to 30 cm is small steps.[34] The first impression given by the data is that the bat can distinguish a difference no smaller than about 14 mm in target range under the conditions of this experiment. However, the bat perceives the distance to each target more sharply; its just that these sharper images are blurred by the movements of the bat's head relative to the targets.

Figure 4B shows a good agreement between the shifted or blurred envelope of the (full-wave) rectified crosscorrelation function and the range discrimination performance of the bats. From this agreement one can conclude that the underlying image of a target must be similar at least to the envelope of the crosscorrelation function. Figure 4A carries this agreement further to show that the detailed peak structure of the function is incorporated into the images as well when experimental conditions are favorable. In the range discrimination task, the smallest detectable range difference is about 6 mm after the errors introduced by the bat's head movements are taken into consideration.[12-14] It remains an open question whether the much finer acuity demonstrated in the jitter discrimination experiment applies as well to the range discrimination experiment. The bat's head movements may blur the images, but they may also deprive the bat of the relative phase information needed to perceive the fine structure under the envelope of the crosscorrelation function.[34,39,40] In any event, the practical target-ranging acuity shown in the range discrimination experiment is compatible with the accuracy of the bat's reaching out to seize a flying insect.

Perception of range-extended targets: The experiments described so far are concerned with the bat's ability to use the delay of echoes for determining how far away a real or simulated target is located. The targets are all discrete points along the range axis—that is, each consists of a single reflecting source occupying a unique position in range. Futhermore, each of these targets is a separate target to the bat. In the echo jitter discrimination experiment (Figure 4A), the target simulator presented the bat with only one echo for each sonar emission; the bat had to observe the echoes returned for a number of successive emissions to gather enough information to perform the task, and the bat's memory for distance from one emission to the next obviously must play a crucial role for the experiment to work.[35] In the target range discrimination experiment (Figure 4B), the two targets were presented simultaneously but separated by a viewing angle of 40°, so the bat had to scan each target in succession to decide which was nearer.[38] Here, too, the bat's memory for distance must be important. The separateness of each target to the bat in the range discrimination task has been confirmed by using a target simulator to ensure that the bat only receives echoes from the particular target it is pointing its sounds

Figure 4

Graphs comparing the performance of the big brown bat, Eptesicus fuscus, in different experiments involving perception of target range (data points with dashed curves labeled Bat) with the crosscorrelation functions (XCor) for the emissions and the echoes from the target (solid curves).

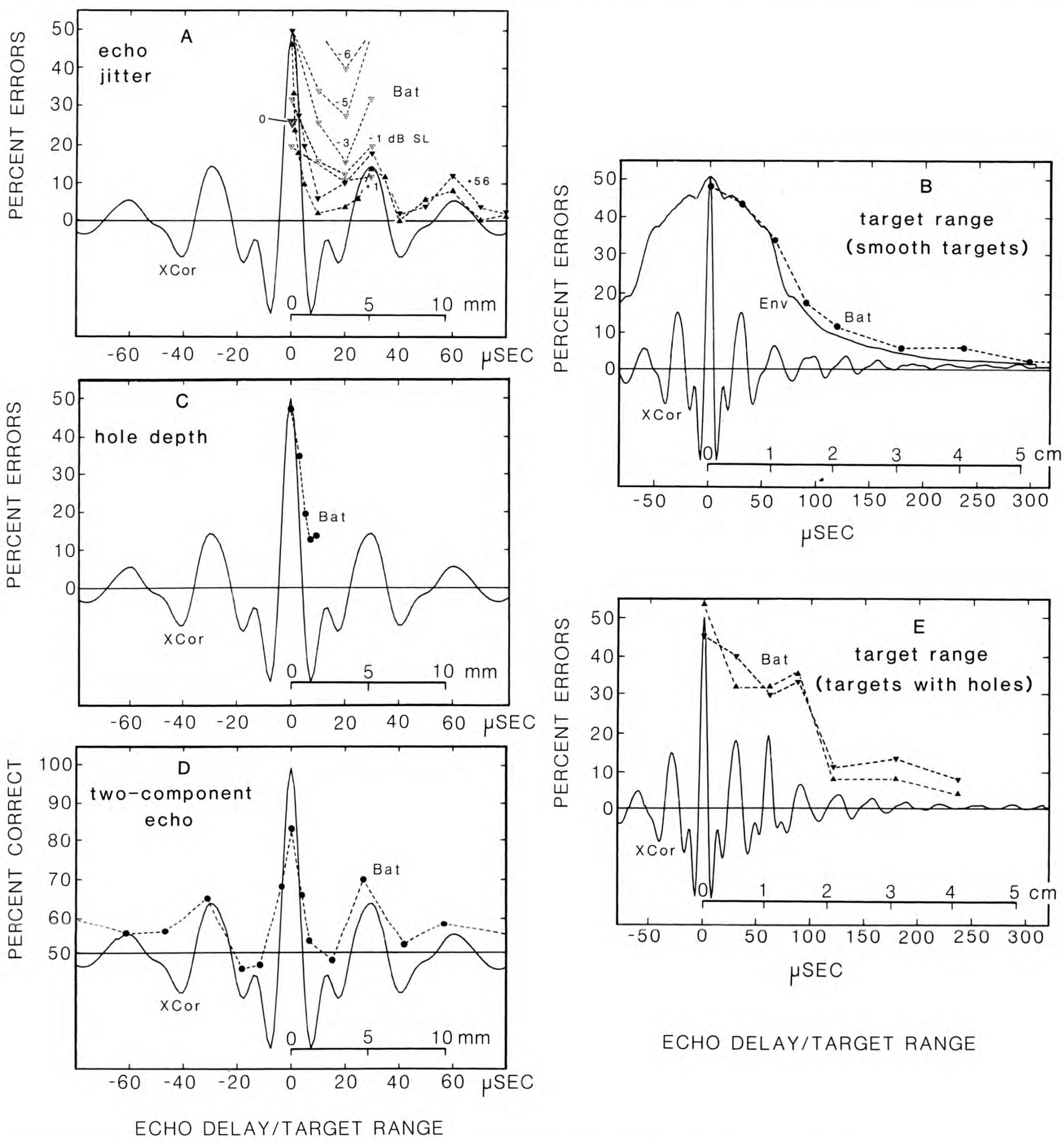

towards.[5] The data shown in Figures 4A and 4B thus represent the accuracy of time-measuring processes in the bat's hearing. They also represent the accuracy of absolute range comparisons made by the bat. Each target's range is determined separately for comparison with the range of another target, whether from one echo to the next in the jitter discrimination experiment or from one set of echoes to another in the range discrimination task. Because each stimulus echo is presented in isolation from others—that is, the echo does not overlap with others—no spectral cues are generated within echoes that can substitute for the use of temporal cues by the bat (see below). It is not yet known whether the bat's head movements do more than merely blur the image in Figure 4A to obtain the data in Figure 4B. Perhaps the fine structure of the image is lost, too.

For the bat to determine differences in distance to parts of a target amounts to perception of the range profile of the target, or the extension of the target along the range axis, as an acoustic version of target shape. Most flying insects only subtend an angle of about 0.5 to 4° at distances of 0.5 to 1 meter, when the bat most likely is making judgments about target shape related to the interception of prey.[36,41] The horizontal width of the image of a target to *Eptesicus fuscus* is about 3°.[23,24] and the vertical width is about 6°.[42] While this directional acuity is adequate to track and intercept prey,[15] it is not sufficient to perceive the distribution of reflecting sources within an insect-sized target along the horizontal and vertical axes. It thus is probable that the entire perceptual attribute of target shape to an echolocating bat is defined in terms of the range profile of objects. To usefully distinguish among different objects whose total size is only from one to several centimeters, the bat would need to perceive the separation of glints along the range axis with an acuity of better than a millimeter or so, and this is what the results of the jitter discrimination experiment reveal to be possible. The jitter task is artificial and unnatural, but so is the question it is intended to answer. By making judgments of the relative distance to the parts of a complex target, the bat could bring its fine range acuity to bear on a biologically relevant task in which its own movements do not disrupt the crucial distance to be determined. The distance to the target as a whole would change as the bat moves closer, but the distance between the parts of the target would not. Only the target's own movements will affect this relative distance, which could indicate that the target is itself alive.

The acuity of perception of the range profile of targets by echolocating bats has been measured in two-choice discrimination tasks similar to those described above. The bat is presented with two targets that contain reflecting surfaces separated by different distances and is trained to respond to the target with the larger or the smaller separation. The bat receives two closely-spaced echo components from each target and implicitly must determine which target reflects double echoes having the greater or the lesser separation in time. The echolocation sounds of the species of bats used in these experiments are typically between 0.5 and 1.5 msec long, whereas the time separations to be discriminated are only a few tens of microseconds, so the double echoes in fact consist of two almost entirely overlapping replicas of the emitted signals impinging on the targets. This overlap generates several acoustic effects which the bat could use to perceive the target's range profile.

The type of target introduced to study range profile discrimination by bats is a flat plate with holes of a fixed depth drilled part-way into its front surface.[43] The target reflects two discrete echo components when it is oriented to face the bat—one component from the front surface and one component from the bottoms of the holes. The bat is trained to discriminate between a target having holes of one particular depth, such as 8 mm, and each of a series of targets having holes of different depths, ranging from 6.5 to 8 mm, for example. Figure 5 shows a bat in a hole-depth discrimination experiment as its selects one of the targets for its response.

Other kinds of targets have been used in experiments on the perception of target shape by bats, but it has proved difficult to isolate and identify echo cues unambiguously in these cases.[38,41,44-46] Hole-depth discrimination experiments have been conducted with several bat species.[43,47], and a variant using targets with granular surfaces of different roughness has been tried, too.[48]—all with similar results.

Figure 4C shows the average percentage of errors made by two *Eptesicus fuscus* as they discriminated differences in the depth of holes in targets.[43] The targets themselves were 30 cm away from the bat (see Figure 5), which was trained to respond to a target with holes that were nominally 8 mm deep and not to respond to targets with shallower holes. The graph in Figure 4C thus shows range difference discrimination in the millimeter region around an absolute range of 30 cm. The two bats discriminated the depth of the holes with few errors until the difference in depth fell below about 0.6 mm; for smaller differences they made a substantial percentage of errors. Following the interpretation of Figure 4A and 4B, we can think of the result of the hole-depth discrimination experiment as providing an approximation to the image that the bat perceives of one reflecting surface along the range axis relative to another reflecting surface located about a centimeter away. This image evidently is about a millimeter wide.

Figure 4D shows the percentage correct performance of one *Eptesicus* discriminating a double echo from a single echo for various separations of the two components of the double echo. The delay of the single echo is 3.3 msec, corresponding to a distance of 57 cm, and the added, second glint in the double echo varies around this fixed center value. The curve traces the bat's ability to perceive the presence of the double glint, whether it is manifested as a stronger echo for zero glint separation, or as a complex echo for various time separations larger than zero. The bat is capable of easily perceiving a difference between zero separation and a very small separation of only 3.75 μ sec, and larger separations vary in their perceptual salience in a cyclical fashion. The bat's performance stabilizes at close to chance levels of correct responses for separations larger than about 60 μ sec in either direction. The main point to make from the data in Figure 4D is that a glint separation of only a few microseconds is perceptible to the bat. (The apparently paradoxical effect that relatively large separations of 40 to 80 μ sec are less readily perceived than very small separations is a consequence of mutual masking between the two glints.[5] When the separation exceeds about 200 μ sec, the bat's performance again rises to 90% correct or better.) A closer simulation of the hole-depth discrimination experiment has also been conducted.[48] The results show an acuity slightly better than for real targets.

The equivalent of phase coherence exhibited in the data from the echo jitter discrimination experiment (Figure 4A) and the hole-depth and glint-separation discrimination experiments (Figures 4C and 4D)show that the relative immunity of the target's absolute range to head-movement artifacts from one echo to the next in the jitter task has its counterpart in the way one glint acts as a reference for the other glint in the experiments with complex targets. For now, the remaining question to ask about targets that are extended in range is whether their distribution along the range axis—which the bat can perceive as a range difference with millimeter acuity— has an effect on the bat's ability to determine the absolute distance to the entire complex target. Does the bat perceive the target to be at the average range of the multiple glints, or does the absolute target-ranging process pick up the existence of the individual glints themselves? To examine this question, bats were trained in the same target ranging task used to collect the data shown in Figure 4B, but the targets were those from the hole-depth discrimination experiment. Instead of choosing the target that has the deeper holes, the bat must choose the target that is nearer, but now the targets have holes in their front surfaces. The particular targets used for this range discrimination experiment both have holes that are 8 mm deep.

Figure 4E shows the percentage of errors made by two *Eptesicus fuscus* as they discriminate between a target with 8-mm holes at a distance of 30 cm and another target with 8-mm holes located at various distances from 25 cm to 30 cm during different stages of the experiment. These results are different in one important respect from the results of the range discrimination experiment with smooth targets (Figure 4B). When discriminating the distance to targets that each present a single reflecting surface, the bat makes relatively few errors if the difference between the nearer and farther targets is more than 10 mm. However, when discriminating between nearer and farther targets that each present two distinct reflecting surfaces, the bat makes a substantial number of errors as long as the difference in distance is small enough to keep the two extended targets nearly overlapping in range. As soon as the difference in distance separates the two targets enough that one target's extent along the range axis is clear of the other target's, the bats make few errors in the discrimination. In Figure 4E the bats experience difficulty in distinguishing between the targets with holes for a range difference of as much as 15 mm, which would have been an easy task with smooth targets. The holes are 8 mm deep, which extends each target along the range axis by 8 mm. For these two targets to be far enough apart that they are as distinguishable as smooth targets separated in range by only 10mm, the targets with holes would have to be at least 18 mm apart.

Figure 5

A drawing showing a bat making its response in a two-choice hole-depth discrimination experiment. The left target has 8-mm holes in the surface facing the bat. The bat is in the act of crawling onto the left arm of the Y-shaped platform to register its choice of the left target.

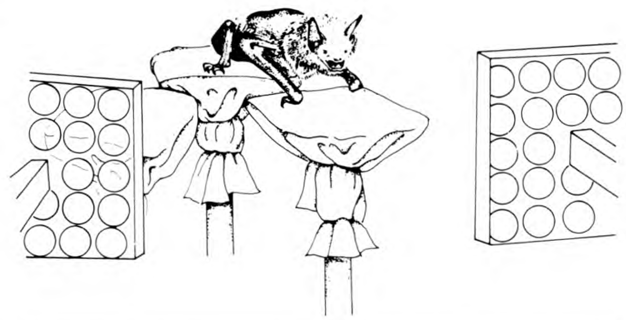

Representation of Echoes and Images

The data in Figure 4A-E illustrate how information about the distance to sonar targets or to parts of targets manifests itself in the images that bats perceive. The collective evidence from these experiments, which explore several different aspects of the perception of target range, is that the bat perceives an image of a single reflecting source along the range axis that corresponds to the crosscorrelation function between sonar emissions and echoes. This is the *ambiguity function* described in radar and sonar theory.[39] The correspondence between the image and this function is only evident if some means are used to stabilize the distance to targets over the short intervals of time from one sonar emission to the next or if the bat is asked to determine the distance between two reflecting sources that constitute a single, complex target.

However, if the bat's movements during the experiment disrupt the stability of the distance to targets while range judgments are in progress, the fine structure of the crosscorrelation function may disappear from the image, leaving only the envelope of this function as the image of a target. The fine range acuity revealed in echo jitter and hole-depth discrimination experiments probably is the basis for the bat's perception of the shape of targets, whereas the coarser acuity revealed in target range discrimination experiments probably illustrates the accuracy of ordinary target range perception. The bat's efforts to reach out and capture targets at the end of the pursuit maneuver are associated with this coarser acuity.

The Display of Target Range

The fine acuity of target ranging achieved in the jitter discrimination experiment depends solely upon the bat's judgments of the delay of echoes. The stimuli are presented one-at-a-time, with no opportunity for echoes to overlap and generate spectral cues for the discrimination. In situations where the delay of individual echoes carries the critical information the bat uses to perform a target ranging task, physiological evidence indicates that the neural computations which create the images are carried out in the time domain. The FM sweeps of individual sonar signals and echoes are represented in a spectrogram-like format within the bat's auditory system.[7,37,49] Figure 6 provides an idealized illustration of the neural spectrogram representations for a sonar emission and an echo from a target at three stages of pursuit (see Figures 1 and 2). The FM sweeps of emissions and echoes are encoded by the time-of-occurrence of nerve impulses distributed across different frequency-tuned channels.[37] The structure of each emission and each echo is represented by the shape of the corresponding volley of impulses across different channels, while the delay of echoes is represented by the interval between impulses evoked by emissions and impulses evoked by echoes within each channel. Echo delay is preserved at this introductory level of the auditory system as the delay of one spectrogram after another.

At higher levels of the bat's auditory system, the time-interval between the spectrogram of each emission and the spectrogram of an echo is transformed into a spatial display of target range.[50-52] The distance to a sonar target is represented on the surface of the auditory cortex by the site of neural activity on a topographic target range "map". The individual neurons in this map respond selectively to echoes falling in a certain span of delays, and the collective activity of all these neurons provides a spectrum of delay selectivity that extends from several centimeters to several meters. Figure 7 illustrates target-range tuning curves for neurons of this type. The anatomical distribution of range-tuned neurons is systematic; adjacent points along the range axis are represented by neurons best tuned to those points and located in adjacent positions on the map. For the bat to perform absolute range judgments, some sort of neural map seems necessary.[53] However, the neural target-range tuning curves appear quite broad in comparison to the acuity of target range discrimination, which is in the region of a centimeter, to say nothing about the acuity of echo jitter discrimination, which is equivalent to a range acuity of a millimeter or less. It seems likely that the image of a target is represented by the activity of a population of neurons within the map as whole, and that some mechanism must be able to "read" the map to recover an image that is sharper than can be observed at the level of any one neuron.

Figure 6

An idealized illustration of the pattern of impulses that would be expected to occur in auditory nerve fibers when stimulated by a single sonar emission (beginning at time zero) and a sonar echo during the search (delay of 20 msec), approach (delay of 6 msec), and terminal (delay of 2.5 msec) stages of pursuit.[37] The vertical frequency axis shows the frequencies to which hypothetical auditory neurons are tuned. Each dot represents a nerve discharge.

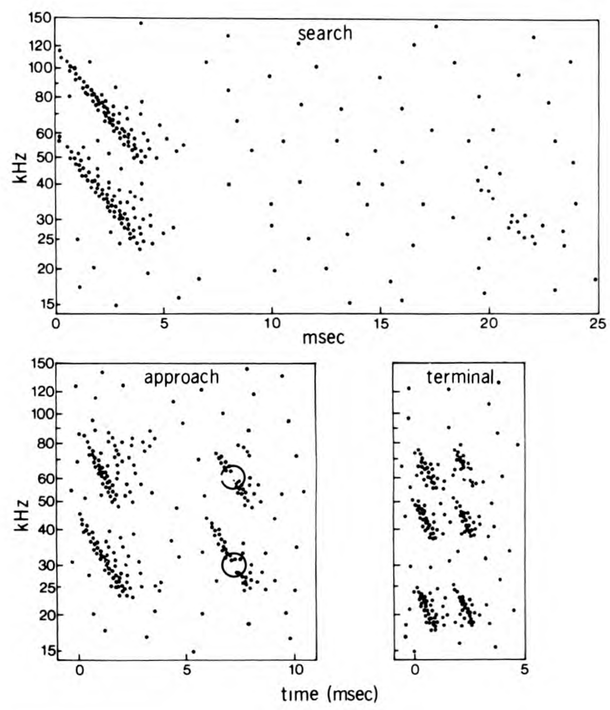

An understanding of the bat's sonar receiver first depends upon learning how spectrograms can be used to obtain crosscorrelation functions.[34] A theoretical analysis of the information contained in spectrograms reveals that the envelope of the crosscorrelation function can be computed by spectrogram correlation.[54,55] If care is taken to preserve phase information at least at one frequency in the spectrograms for emissions and echoes, the fine structure of the crosscorrelation function can be computed, too. Figure 4A shows that the image of a target corresponds to the half-wave-rectified crosscorrelation function. The bat behaves as though the output of the target-ranging component of its sonar receiver takes the form of this function. How can such a display be achieved and how can it be read?

Figure 7

Target-range tuning curves from the "range map" on the auditory cortex of the mustache bat, Pteronotus parnellii.[50]

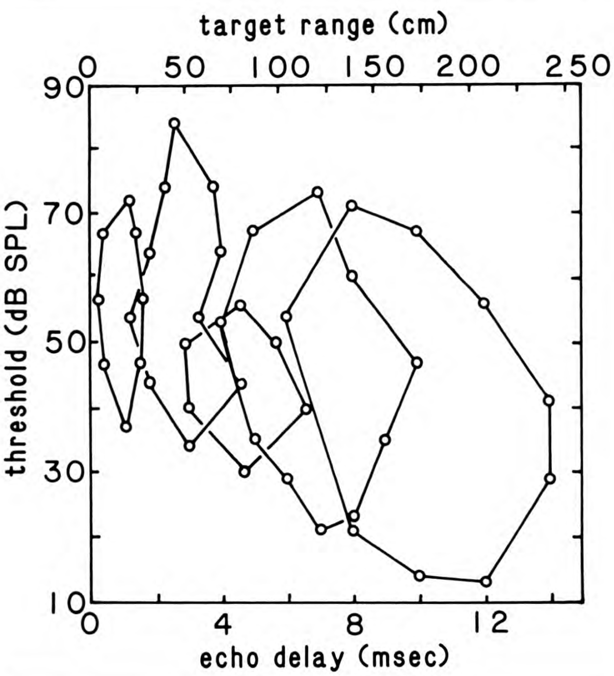

The difficulty encountered in trying to relate the coarse accuracy of target range tuning curves of neurons (Figure 7) to the fine acuity of target ranging (Figures 4A and even 4B) arises from the same data that suggest some kind of correlation image represents targets. Perhaps the mechanism that reads the neural map can be made to reveal itself in the nature of the image that the bat perceives. The critical computations in spectrogram correlation involve keeping track of the time-interval between a nerve impulse representing the emission and a nerve impulse representing an echo within each of the many frequency channels used to develop the spectrogram representations themselves (Figure 6). The bat's auditory system explicitly converts the time-delay of echoes into a topographic representation, and the information needed to create this topographic representation is carried by the timing of nerve impulses representing emissions and echoes in each frequency channel. The cortical target range tuning curves are not frequency-specific, so they probably represent a topographic display of neural timing information integrated across many frequency channels.[2,50-52] However, they do not represent the timing information itself with the accuracy that ultimately is manifested in the bat's perception of targets, nor indeed in the original neural spectrograms.[49] The conclusion seems inescapable that the transformation of timing information from the spectrograms to the target range tuning curves is only a partial transformation. It is true that a spatial interpolation process may sharpen the image extracted from the map, but it cannot recreate the fine structure that shows up in the image. The timing of impulses in the range-tuned neurons themselves must contribute to the process of reading the target range map. This is another way of saying that the map, although a spatial display of target range, does not express all of the precision of the target ranging system along its spatial axis. Some of this precision remains in and is expressed by the timing of events on the map rather than simply by the location of events on the map. One possible means for incorporating the timing of impulses in range-tuned neurons as part of the map-reading process would be to assign the image of a target to a population of neurons that discharge simultaneously, discarding the information contributed by neurons that discharge too soon or too late with respect to the bulk of the population. This and similar hypotheses about the retrieval of images from the map are presently being explored through physiological experiments in several laboratories.

The Display of Target Shape

In experiments with bats discriminating the depth of holes in targets, the echoes consist of two closely-spaced replicas of the emitted sound. The replicas are separated by relatively short time-intervals. Acoustic measurements of the echoes reflected by targets with 8-mm holes show the separation of echo components to be only about 50 to 60 μ sec. It is theoretically possible to determine the depth of the holes by detecting the presence of two distinct echo components separated in time by 50 to 60 μ sec. However, the bat's sonar sounds are about one millisecond long in this experiment, so the echoes actually consist of almost completely overlapping replicas of the original emissions. The presence of two closely-spaced components would be concealed within the slightly longer waveform of the echo taken as a whole. It is still possible to observe the presence of two echo components in the crosscorrelation function for the echoes, and the data shown in Figure 4C-E indicate that the bat's image of a complex target corresponds closely with this function. The difficulty is that, unlike the situation in target ranging experiments, the critical auditory representation of complex echoes probably is spectral in nature.

The spectrograms of sonar emissions and echoes (Figure 6) are built up within frequency channels that are originally established at the time sounds are transduced into nerve impulses by the inner ear.[56] Each frequency channel is defined by the tuning properties of the receptor cell that activates the first neuron in the chain of neurons that constitutes the frequency channel itself. In bats, the band-pass filters that define each channel are moderately sharply tuned to their individual characteristic (center) frequencies, with low-frequency slopes of about 110 dB per octave and high-frequency slopes of about 260-290 dB per octave.[57] When an FM echolocation sound or echo passes through such a filter, the waveform that emerges is several hundred microseconds long and provides no cues in its time structure about whether just one echo or several echo components are present with separations as small as 50 μ sec. Instead, the *amplitude* of the waveform that emerges from the filter represents the magnitude of the spectral component defined by the filter's characteristic frequency. Two closely-spaced echo components interfere with or reinforce each other in the many channels that make up the whole receiver. For echo components separated by short intervals of up to about 100 μ sec, the bat's auditory system probably represents the structure of the echoes by their spectrum instead of by their timing.[43,58] The spectrum will have notches at frequencies determined by the time separation of the echo components. Thus, the depth structure or range profile of the target is expressed in terms of the amplitude of the echo at different frequencies across the neural spectrogram (Figure 6). This is in contrast to the delay of echoes after emissions, which is directly represented by the time-interval between the spectrogram of the emission and the spectrogram of the echo.

In the spectrograms shown in Figure 6, the shape of the target appears as a variation in the amplitudes represented along the FM sweep for the echo. Nevertheless, the results of the target ranging experiment with targets that have holes in their surfaces (Figure 4E) show that this spectral information somehow ultimately makes its way into the same range image that represents the delay of echoes. The spectrally-represented range profile is apparently perceived in terms of its equivalent effect on the crosscorrelation function of echoes rather than as a separate "spectral" feature of targets that is distinct from target range. The evidence is strong that the images of targets in echo jitter and target range discrimination experiments correspond to crosscorrelation functions that must have been computed from spectrograms such as those shown in Figure 6. The most parsimonious explanation for the appearance of spectrally-represented echo structure in the same crosscorrelation functions is that the amplitude of each frequency component enters into the computation along with the time-of-occurrence of each frequency component. Only a spectrogram correlation process seems able to integrate both range profile and absolute range smoothly into a single image. It remains to be seen how this signal-processing model actually works in the bat's brain. Does the spectrally-coded information appear in the neural responses evoked by complex echoes in the target range map, or is some fundamentally different display of shape created apart from the range map?

Biography

Dr. Simmons presently is a Professor in the Section of Neurobiology and in the Department of Psychology at Brown University, having previously been a member of the Department of Biology at the University of Oregon and the Department of Psychology and Program in Neural Sciences at Washington University in St. Louis. While a graduate student with Professor E. G. Wever, at Princeton University, he began ONR-sponsored research on bats to identify the acoustic features of echoes that contribute to the formation of spatial images of targets. This research has led to both theoretical and experimental work on the development of hybrid time/frequency domain signal-processing techniques.

References

1. Griffin, D. R. *Listening in the Dark,* Yale Univ. Press, New Haven, CT (1958). (Reprinted by Cornell Univ. Press, Ithaca, NY, 1986).

2. Suga, N., The extent to which biosonar information is represented in the bat auditory cortex, in: *Dynamic Aspects of Neo-Cortical Function,* G.M. Edelman, W.E. Gall, and W.M. Cowan, eds., Wiley, New York, pp. 315-373 (1984).

3. Hill, J. E., and Smith, J. D., *Bats—A Natural History,* Univ. of Texas Press, Austin, TX (1984).

4. Novick, A., Acoustic orientation, in: *Biology of Bats,* Vol. III, W.A. Wimsatt, ed., Academic Press, New York, pp. 73-287 (1977).

5. Simmons, J. A., *The Sonar of Bats,* Princeton Univ. Press, Princeton, NJ (in press).

6. Neuweiler, G., Bruns, V., and Schuller, G., Ears adapted for the detection of motion, or how echolocating bats have exploited the capacities of the mammalian auditory system, *J. Acoust. Soc. Am., 68,* 741-753 (1980)

7. Suga, N., Feature extraction in the auditory system of bats, in: *Basic Mechanisms in Hearing,* A.R. Møller, ed., Academic Press, New York, pp. 675-744 (1973).

8. Fenton, M. B., Echolocation: Implications for ecology and evolution of bats, *Quart. Rev. Biol., 59:* 33-53 (1984).

9. Schnitzler, H.-U., and Henson, O. W., Jr., Performance of airborne animal sonar systems: I. Microchiroptera, in: *Animal Sonar Systems,* R.-G. Busnel and J.F. Fish, eds., Plenum, New York, pp. 109-181 (1980).

10. Simmons, J.A., Fenton, M. B., and O'Farrell, M. J., Echolocation and pursuit of prey by bats, *Science, 203:* 16-21 (1979).

11. Schnitzler, H.-U., Menne, D., Kober, R., and Heblich, K., The acoustical image of fluttering insects in echolocating bats, in: *Neuroethology and Behavioral Physiology; Roots and Growing Points,* F. Huber and H. Markl, eds., Springer, Berlin, pp. 235-250 (1983).

12. Simmons, J. A., and Grinnell, A. D., The performance of echolocation: acoustic images perceived by echolocating bats, in: *Animal Sonar Systems,* P. Nachtigall, ed., Plenum, New York, (in press).

13. Simmons, J. A., and Stein, R. A., Acoustic imaging in bat sonar: Echolocation signals and the evolution of echolocation, *J. Comp. Physiol., 135:*61-84 (1980).

14. Simmons, J. A., Howell, D.J., and Suga, N., Information content of bat sonar echoes, *Am. Sci., 63:*204-215, (1975).

15. Webster, F. A., and Brazier, O. G., Experimental studies on target detection, evaluation and interception by echolocating bats, Technical Report No. AMRL-TR-65-172, Clearinghouse for Federal Scientific and Technical Information, Springfield, VA (1965).

16. Webster, F. A., and Brazier, O. G., Experimental studies on echolocation mechanisms in bats, Technical Report No. AMRL-TR-67-192, Clearinghouse for Federal Scientific and Technical Information, Springfield, VA (1968).

17. Schnitzler, H.-U., Kalko, E., Miller, L., and Surlykke, A., The echolocation and hunting behavior of the bat, *Pipistrellus kuhli, J. Comp. Physiol.* (in press).

18. Trappe, M., Schnitzler, H.-U., Doppler-shift compensation in insect-catching horseshoe bats, *Naturwiss, 69:*193-194 (1982).

19. Henson, O. W., Jr., Bishop, A. L., Keating, A. W., Kobler, J. B., Henson, M. M., Wilson, B. S., and Hansen, R. C. Biosonar imaging of insects by *Pteronotus p. parnellii,* the mustached bat, *Natl. Geog. Res., 3:*82-101 (1987).

20. Novick, A., and Vaisnys, J. R., Echolocation of flying insects by the bat, *Chilonycteris parnellii, Biol. Bull., 127:*478-488 (1964).

21. Novick, A., Pulse duration in the echolocation of insects by the bat, *Pteronotus, Ergebnisse Biol., 26:*21-26 (1963).

22. Novick, A., Echolocation of flying insects by the bat, *Chilonycteris psilotis, Biol. Bull., 128:*297-314 (1965).

23. Masters, W. M., Moffat, A. J. M., and Simmons, J. A., Sonar tracking of horizontally moving targets by the big brown bat, *Eptesicus fuscus, Science, 228:*1331-1333 (1985).

24. Simmons, J. A., Kick, S. A., Lawrence, B. D., Hale, C., Bard, C., and Escudié, B., Acuity of horizontal angle discrimination by the echolocating bat, *Eptesicus fuscus, J. Comp. Physiol., 153:*321-330 (1983).

25. Lawrence, B. D., and Simmons, J. A., Measurement of atmospheric attenuation at ultrasonic frequencies and the significance for echolocation by bats, *J. Acoust. Soc. Am., 71:*484-490 (1982).

26. Webster, F. A., and Griffin, D. R., The role of the flight membranes in insect capture by bats, *Anim. Behav., 10:*332-340 (1962).

27. Trappe, M., Verhalten und Echoortung der Grossen Hufeisennase *(Rhinolophus ferrumequinum)* beim Insektenfang, Ph.D. Thesis, Universität Marburg (1982).

28. Griffin, D.R., The importance of atmospheric attenuation for the echolocation of bats *(Chiroptera), Anim. Behav, 19:*55-61 (1971).

29. Pye, J. D., Echolocation signals and echoes in air, in: *Animal Sonar Systems,* R.-G. Busnel and J. F. Fish, eds., Plenum Press, New York, pp. 309-353 (1980).

30. Neubauer, W. G., *Acoustic Reflection from Surfaces and Shapes,* Naval Research Laboratory, Washington, D.C. (1986).

31. Kick, S. A., Target detection by the echolocating bat, *Eptesicus fuscus, J. Comp. Physiol. 145:*431-435 (1982).

32. Dalland, J. I., Hearing sensitivity in bats, *Science, 150:*1185-1186 (1965).

33. Cahlander, D. A., McCue, J. J. G., and Webster, F. A., The determination of distance by echolocating bats, *Nature, 201:*544-546 (1964).

34. Simmons, J. A., The resolution of target range by echolocating bats, *J. Acoust. Soc. Am., 54:*157-173 (1973).

35. Simmons, J. A., Perception of echo phase information in bat sonar, *Science, 204:*1336-1338 (1979).

36. Kick, S. A., and Simmons, J. A. Automatic gain control in the bat's sonar receiver and the neuroethology of echolocation, *J. Neurosci., 4:*2725-2737 (1984).

37. Simmons, J. A., and Kick, S. A., Physiological mechanisms for spatial filtering and image enhancement in the sonar of bats, *Ann, Rev. Physiol., 46:*599-614 (1984).

38. Simmons, J. A., and Vernon, J. A., Echolocation: discrimination of targets by the bat, *Eptesicus fuscus, J. Exp. Zool., 176:*315-328 (1971).

39. Woodward, P. M., *Probability and Information Theory, with Applications to Radar,* 2nd Edition, Pergamon, New York (1964).

40. Menne, D., and Hackbarth, H., Accuracy of distance measurement in the bat *Eptesicus fuscus:* Theoretical aspects and computer simulations, *J. Acoust. Soc. Am., 79:*386-397 (1986).

41. Griffin, D. R., Friend, J. H., and Webster, F. A., Target discrimination by the echolocation of bats, *J. Exp. Zool., 158:*155-168 (1965).

42. Lawrence, B. D., and Simmons, J. A., Echolocation in bats: The external ear and perception of the vertical positions of targets, *Science, 218:*481-483 (1982).

43. Simmons, J. A., Lavender, W. A., Lavender, B. A., Doroshow, C. A., Kiefer, S. W., Livingston, R., Scallet, A. C., and Crowley, D. E., Target structure and echo spectral discrimination by echolocating bats, *Science, 186:*1130-1132 (1974).

44. Ajrapetjantz, E., and Konstantinov, A. I., *Echolocation in Nature,* Nauka, Leningrad (English translation, Joint Publications Research Service, Arlington, VA) (1974).

45. Bradbury, J. W., Target discrimination by the echolocating bat *Vampyrum spectrum, J. Exp. Zool., 173:*23-46 (1970).

46. Griffin, D. R., Discriminative echolocation by bats, in: *Animal Sonar Systems: Biology and Bionics,* Vol. I, R.-G. Busnel, ed., Laboratoire de Physiologie Acoustique, Jouy-en-Josas, France, pp. 273-300 (1967).

47. Habersetzer, J., and Vogler, B., Discrimination of surface-structured targets by the echolocating bat *Myotis myotis* during flight, *J. Comp. Physiol., 152:*275-282 (1983).

48. Schmidt, S., Discrimination of target surface in the echolocating bat, *Megaderma lyra,* in: *Animal Sonar Systems,* P. Nachtigall, ed., Plenum, New York (in press).

49. Bodenhamer, R. D., and Pollak, G. D., Time and frequency domain processing in the inferior colliculus of echolocating bats, *Hearing Res., 5:*317-355 (1981).

50. O'Neill, W. E., and Suga, N., Encoding of target-range information and its representation in the auditory cortex of the mustached bat, *J. Neurosci., 47:*225-255 (1982).

51. Suga, N., and Horikawa, J., Multiple time axes for representation of echo delays in the auditory cortex of the mustached bat, *J. Neurophysiol., 55:*776-806 (1986).

52. Sullivan, W. E., Neural representation of target distance in auditory cortex of the echolocating bat, *Myotis lucifugus, J. Neurophysiol., 48:*1011-1032 (1982).

53. Simmons, J. A., and Lavender, W. A., Representation of target range in the sonar receivers of echolocating bats, *J. Acoust. Soc. Am., 60:*S5 (1976).

54. Altes, R. A., Detection, estimation and classification with spectrograms, *J. Acoust. Soc. Am., 67:*1232-1246 (1980).

55. Altes, R. A., Echo phase perception in bat sonar? *J. Acoust. Soc. Am., 69:*505-508 (1981).

56. Møller, A. R., *Auditory Physiology,* Academic Press, New York (1983).

57. Suga, N., and Jen, P. H.-S., Further studies on the peripheral auditory system of CF-FM bats specialized for fine frequency analysis of Doppler-shifted echoes, *J. Exp. Biol., 69:*207-232 (1977).

58. Beuter, K. J., A new concept of echo evaluation in the auditory system of bats, in: *Animal Sonar Systems,* R.-G. Busnel and J. F. Fish, eds., Plenum, New York, pp. 747-761 (1980).

SEMICONDUCTING DIAMOND TECHNOLOGY

By Max N. Yoder
Office of Naval Research

The superlative properties of tetrahedrally-bonded carbon crystals (diamonds) have been known for over a decade. In most respects they exceed those of all other semiconductors. Described here is a brief history of the search for a synthetic diamond followed by a description of state-of-the-art approaches. Comparisons of diamond properties with those of other semiconductors are shown in the context of electronic devices and electromagnetic systems advantages that may be engendered by diamond.

Background

Diamonds have been known since biblical times, but artifact diamonds are comparatively new. As early as 1797, the diamond was known to consist solely of carbon. Various individuals have been credited with the distinction of being the first to have synthetically produced a diamond, but few have been verified. Among the earliest is C. Cagniard de la Tour in 1832, but the products of his endeavors are not to be found today. Those supposedly made by J. B. Hanney of lithium metal, bone meal, and mineral oil sealed and heated in a wrought iron tube are currently on display in the British Museum.

His 1880 fete was supposedly followed by Henry Moisson using his new invention of the electric arc furnace. This 1893 endeavor used sugar charcoal in molten iron followed by quenching in water. Percy Bridgman of Harvard University spent a lifetime pursuing diamond without success although he was most successful in synthesizing other crystals and developing high-pressure apparatus for which he received a Nobel prize in 1948. Gibbs showed that graphite could not turn into diamond unless the "thermodynamic potential" of diamond was less than that of graphite. The mathematical expression for the thermodynamic potential showed that if the pressure could be raised high enough, graphite would "receive thermodynamic permission" to transform to diamond. Unfortunately, pressures exceeding 250,000 p.s.i. were required at moderate temperatures. This knowledge led to the Belt High Pressure Apparatus at General Electric wherein pressures of 2,500,000 p.s.i. and temperatures of 1,800 degrees Celsius could be sustained for several minutes. With these techniques, over 150 tons of artifact diamonds have now been made.

Bulk stones of indeterminate and irregular size did not, however, lend themselves to hard surfacing tools, the creating of optical windows, or the fabrication of diamond semiconductors. Chemical vapor deposition (CVD) came into its own in the late 1950's, and with it Professor John Angus of Case Western Reserve University began his open flow CVD depositions in the 1961-68 time period. This work was mostly known for the diamond-like hydrocarbons it produced. B.V. Derjaguin of the USSR initiated closed tube CVD in the 1970's with limited success. A real stimulus for the synthesis of semiconducting diamond was the 1975 paper by D.K. Ferry wherein the electrical properties of diamond were placed in perspective with those of other semiconductors.[1]

Microwave plasma work of the 1960's by F.J. Vastola and later by B.E. Knox of The Pennsylvania State University were adapted by the research team established at the National Institute for Research in Inorganic Materials in Japan in mid 70's. There S Matsumoto and Y. Kato synthesized the first non-hydrocarbon diamond films on various materials. This pioneering work stimulated other Japanese efforts and there are now over 30 different organizations in Japan pursuing the synthesis of diamond. These pursuits have generated over 200 patents from 1980-86.

In the U.S., the largest government funded efforts exist at The Pennsylvania State University, the North Carolina State Univesity, and at the Research Triangle Institute. An increasing number of privately funded efforts are also underway. Virtually all current contracts in the field are being administered by the Office of Naval Research.

General Properties

Semiconducting diamond is an indirect gap semiconductor having a bandgap of 5.45 electron volts. The conduction band resembles that of silicon. The purest natural diamonds have resistivities up to 10^{16} ohm-cm and have negligible amounts of nitrogen or boron. Boron is known to act as an acceptor in diamond and to provide a blue color while nitrogen is a donor and provides a yellow tint. Natural diamond is not homogeneously doped; Nd-Na typically varies by as much as ten-fold over a small area. Electron mobilities in the vicinity of 1,800-2,200 cm^2/ Volt-seconds have been measured at room temperature, but the deep donor levels inhibit conduction at lower temperatures.[2,3] Electron charge carrier velocity is thought to saturate at about 2.3×10^7 cm/sec beginning at electric fields as low as 20×10^3 Volts/ cm.[1]

While this value is about equal to that of the peak of the gallium arsenide static velocity field relationship, diamond has no negative differential conductivity. This means that charges can travel along a very long path without gaining mass and slowing. Stated differently, electron devices can be internally and integrally cascoded (charge carrier paths connected in series) without need for highly doped low electric field regions to "retrieve" the electrons from their upper subsidiary conduction band high mass state. Several benefits accrue from this property. Chief among them is that the electrons need not be slowed to near zero velocity between integrally connected devices. Thus, even though the electron mobility may not be equal to that of competing III-V materials, the average velocity over a two device path can be considerably higher in diamond. The absence of a highly doped, retarding electric field region between two devices also significantly reduces quantum electron reflection which can account for up to 30% of electrons being reversed in direction as would be required in a III-V device. With an electric field breakdown strength of 10^7Volts/cm, the area under the velocity-field curve for diamond is considerably larger than that of any other semiconductor. This directly correlates to high values for power-frequency products. In fact, the Johnson figure-of-merit (power-frequency squared-impedance product) for diamond is 8,200 times that of silicon and about 1,000 times that of gallium arsenide as shown in Table 1. Another factor contributing to high figure-of-merit is a dielectric constant of 5.5 which is about half of that of conventional semiconductors. With a thermal conductivity 5 times that of copper (20 times that of silicon), the packing density can also be high. The Keyes figure-of-merit for diamond is 32 times that of silicon and exceeds that of all other semiconductors as is shown in Table 2. A hole mobility of 1900 cm^2/Volt-second is exceeded only by germanium in conventional semiconductors. It is interesting to note that this hole mobility exceeds that of the electron mobility of silicon. If complementary devices are constructed, the p-channel need not be excessively larger than the n-channel to equate output currents.

Table 1

Johnson figure of merit for selected semiconductor materials.

	E_B (VOLTS/CM)	V_{SAT} (CM/SEC)	$\frac{E_B V_{SAT}}{\pi}$ (VOLTS/SEC)	$P_M F_L^2 Z_L$ $\frac{\text{WATT - OHM}}{\text{SEC}^2}$	RATIOS TO SILICON DIMENSIONLESS
SI	3×10^5	1.0×10^7	9.5×10^{11}	9.0×10^{23}	1.0
GAAS	4×10^5	2.0×10^7	25.0×10^{11}	62.5×10^{23}	6.9
INP	6×10^5	2.0×10^7	38.0×10^{11}	144.4×10^{23}	16.0
A SIC	40×10^5	2.0×10^7	250.0×10^{11}	$6{,}250 \times 10^{23}$	694.4
B SIC	40×10^5	2.5×10^7	320.0×10^{11}	$10{,}240 \times 10^{23}$	1137.8
DIAMOND	100×10^5	2.7×10^7	859.4×10^{11}	$73{,}856 \times 10^{23}$	8206.0

Table 2

Keyes' figure of merit for selected semiconductors.

MATERIAL	σ_T 300°K	V_{SAT}	K	$\sigma_T \left(\frac{V_{SAT}}{K}\right)^{\frac{1}{2}}$	RATIO
UNITS	W/CM°C	CM/SEC	DIMENSIONLESS	W/CM$^{\frac{1}{2}}$SEC$^{\frac{1}{2}}$°C	
SILICON	1.5	1.0×10^7	11.8	13.8×10^2	1
GALLIUM ARSENIDE	0.5	2.0×10^7	12.8	6.3×10^2	.456
INDIUM PHOSPHIDE	0.7	2.0×10^7	14.0	8.4×10^2	.608
B SILICON CARBIDE	5.0	2.5×10^7	9.7	90.3×10^2	5.8
DIAMOND	20.0	2.7×10^7	5.5	444×10^2	32.2
COPPER	3.98	N/A	N/A	N/A	N/A

Processing

While many semiconductor materials are subject to scratching during handling and processing, diamond is immune to this hazard as it is the hardest of all known materials as shown in Figure 1. Even though hard and virtually imperious to wet chemicals at room temperature, ion-beam-assisted etching rates of up to 200 nanometers/minute have been obtained by Geis.[4] Using a variation of this process, it may be possible to digitally control the etching of diamond to one monolayer at a time. If so, this would provide a degree of control unmatched in any other semiconductor processing technology.

Figure 1

Diamond properties in comparison.

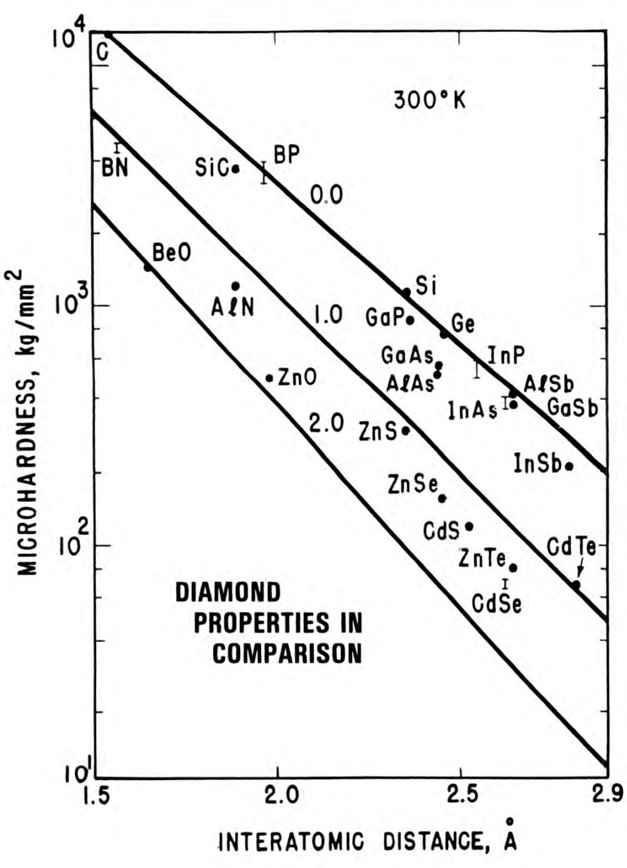

Impurity Doping

The semiconducting nature of natural diamond was first discovered by Custers.[5] Natural diamond is always p-type (type IIb). For many years it was thought that aluminum was the substitutional impurity. Collins and Williams[6] were able to show by Hall effect measurements that the very small concentration of aluminum could not be responsible for the acceptor concentration in natural diamond. Lightowlers and Collins[7] were the first to show boron to be the natural acceptor. Although natural diamonds are not homogeneously doped (therefore rendering Hall measurements difficult), the energy level of boron is generally thought to be 370 millivolts above the valence band. Nitrogen concentrations in natural diamond can reach nearly 1%; as a deep (e.g., 1 eV) donor, it is usually present in sufficient quantity to compensate the boron and aluminum present. Lithium has been shown to be a donor in diamond and can exhibit mobility exceeding 1,000. It is, however, interstitial and may not be useful for high temperature work.

Ohmic contacts to n-type material have proven very difficult. With a bandgap of 5.45 electron volts, one may imagine that virtually every element in the periodic table will exhibit an energy level within the gap. Fortunately, excepting for elements in row 1 of the periodic table, most impurities are physically too large to fit in the diamond lattice. Diamond, being an exceedingly hard material with a very small lattice constant, is virtually impervious to diffusion. There are no known surface diffusion experiments which were undisputedly successful. Wilson[8] indicated that boron may have diffused under high temperature and high pressure, but the experiment was such that the possibility existed of a boron-doped epitaxial layer being formed instead. Wentorf and Darrow[9] indicate the efficacy of ion implantation of nitrogen. Clark and Mitchell cast doubt on the ion implantation experiments.[10] A major problem with ion implantation is that activation temperatures above 1,400 Celsius in vacuum lead to a graphitization of the surface. One approach to circumventing this problem may be to place the diamond surface at a pressure above the graphite-diamond phase transition line.

Carrier Dynamics

Hall effect electron mobilities of up to 3,000 cm^2/volt-second have been measured in natural diamonds.[6,11] Time-of-flight measurements have been conducted in diamond at temperatures from near absolute zero to 1,000K with respective mobilities of 20,000 to 200 cm^2/volt-second for electrons and 20,000 to 100 cm^2/volt-second for holes.[12] Hole velocity tends to saturate at around 10^7/cm second at electric field strengths of 50,000 volts/cm while electron velocity saturation may begin as low as 20,000 volts/cm and reach hard saturation at 100,000 volts/cm. Velocities up to 2.5 x 10^7 have been measured. While shallow donor impurity doping may prove difficult, the possibility of hot electron injection from a nearly lattice matched boron nitrite material of even higher bandgap exists. (See Figure 1.)

Insulating Diamond

With nearly 5.5 electron volts of forbidden bandgap, pure diamond is an excellent insulator at room temperature. Even at temperatures as high as 1,000 Kelvin, free carrier concentrations as low as 10^5 per cubic centimeter are typical. Resistivities of 10^{14} to 10^{16} inverse ohm-cm are typical.

Photoconductivity

There is no measurable photoconductivity in high quality diamond below the band edge. Most natural diamond has an 8 micrometer absorption line (probably due to hydrogen) and (in type la material) absorption is seen between 4.0 and 4.7 eV.

Optical losses, when present, in diamond are almost always lower (in any given portion of the spectrum below the band edge) than in any other material.

Synthesis

Since natural diamond is non-homogeneously doped and not available in large boules, it is not readily adaptable for semiconductor use. Hydrogen and nitrogen in natural diamond limit its usefulness as an optical window, and it is not readily plated onto cutting tools. An incentive therefore exists to synthesize diamond films. In this synthesis, it appears to be broadly accepted that a carbonaceous gas be chosen such that the carbon is sp3 bonded in the gas state and that the carbon is held in this state through the transition from gas to crystal. It is also broadly accepted that the growing diamond crystal surface not be permitted to reconstruct into dangling bonds and that the surface bonds always be terminated with hydrogen so as to preclude pi bonding. A consensus as to how these dual objectives are accomplished has not developed. As growth temperatures above 900 Celsius lead to increasingly larger incorporation of graphitic (pi) bonds, the ideal substrate temperature must be lower than this. At such temperatures, virtually all carbonaceous gases containing exclusive sp3 bonds do not readily pyrolize. An external source of energy is necessary to accomplish three functions: (1) decomposition of the gas into (preferably) CH3 radicals, (2) provide surface migration velocity otherwise supplied by high substrate temperatures, and (3) provide energy sufficient to break the longer ligand bonds of surface impurities without damaging the underlying crystal. These energies are typically derived from noble gas plasmas. The technique in largest use is to immerse the growing film in a plasma of hydrogen, methane, and noble gas. While impressive results have been obtained in this manner, there is a large interdependance among various factors and control; reproducibility is difficult. Changes in plasma energy not only affect the density of methane radicals present, but also the substrate temperature. Ions present may create dislocations in the growing crystal structure. To obtain extra degrees of freedom, remote plasmas are increasingly used. In such an approach, the substrate temperature is independently controlled. Only a noble gas is subjected to the electromagnetic field. The ions created are directed towards the growing film. In the path towards the film, they are first neutralized to form excited metastable state monomers and then permitted to interact with the carbonaceous gas injected immediately above the growth surface. It is thought that the chance of CH2 radicals being created is minimized in this manner. Ultra violet light generated by the plasma may be instrumental in generating unwanted CH and CH2 radicals, although other experiments use UV light in place of metastable state monomers to affect the growth. Although much work remains to be accomplished in diamond thin film growth, there has been limited success at growing single crystalline diamond films both epitaxially and heteroepitaxially.

In summary, diamond has several unique properties which make it the leading candidate for many applications. When considered for use, its hardness, thermal conductivity, voltage breakdown, saturated charge carrier velocity, optical losses, or combinations of these properties significantly exceed that of competing materials. Being of simple structure, an understanding of its nucleation, synthesis, and growth is expected to lead to improvements in related materials as well.

Biography

Mr. Max Yoder is an electronics engineer with the Solid State Electronics Branch of the Office of Naval Research where he supervises programs in semiconductor materials, monolithic microwave integrated circuits, gigabit logic, new electronic device structures, and electromagnetic system applications. He has published and presented many papers in these fields of solid state materials. He is a pioneer in the development of research programs for monolithic microwave devices in the U.S. Currently he manages at ONR the new research program in diamond semiconductor technology.

References

1. Ferry, D.D., "High-field Transport in Wide-bandgap Semiconductors," *Physical Review B,* Vol. 12, No. 6, September 1975.

2. Konorova, E.A. and S.A. Shevxhwmka, *Soviet Physics Semiconductor,* Vol. 1, No. 3, p. 299, 1967.

3. Redfield, A.G., *Physics Review,* Vol. 94, p. 526, 1954.

4. Geis, M., "Diamond Transistor Technology," Diamond Technology Initiative Seminar, Durham, N.C., July 17-18, 1986.

5. Custers, J.H.F., *Physica,* Vol. 20, p. 183, 1954.

6. Collins A.T. and A.W.S. Williams, *Journal of Physics C,* Vol. 4, p. 1789.

7. Lightowlers, E.C. and A.T. Collins, *Diamond Research,* p. 14, 1976.

8. Wilson, W., *Physics Review,* Vol. 127, p. 1549.

9. Wentorf, R. and K. Darrow, *Physics Review,* Vol. 137, p. A1614, 1971.

10. Clark, C. and W.W.J. Mitchell, *Radiation Effects,* Vol. 9, p. 219, 1971.

11. Dean, P.J., E.C. Lightowlers, and D. Wight, *Physics Review,* Vol. A140, No. 1, p. 352, 1965.

12. Nava, F., C. Canali, D. Jacoboni, and L. Reggiani, *Solid State Communications,* Vol. 33, No. 4, p. 475.

13. Markunas, R., "The R.T.I. Diamond Initiative," Diamond Technology Seminar, Durham, N.C., July 17-18, 1986.

Profiles in Science

Dr. Gerald Lucovsky is University Professor of Physics at North Carolina State University, which post he has held since 1979. Prior to that, he was with the Xerox Corporation for many years, where he was Senior Research Fellow and Manager of the Xerox PARC General Sciences Laboratory. Since coming to North Carolina State University, Professor Lucovsky has been a Principal Investigator for the Office of Naval Research, conducting research on bonding defects at semiconductor-insulator interfaces. Also, under ONR support, he has pioneered the area of remote plasma chemical vapor deposition as a technique for the deposition of insulating and semiconducting thin films. This technique has great promise for the preparation of high quality diamond material

Professor Lucovsky is renowned for his research and many publications pertaining to local atomic structure and vibrational properties in disordered solids. Of special note, this research has involved properties of interfaces between semiconductors and amorphous or crystalline insulators. He is also recognized for theoretical calculations of vibrational modes and in chemical bonding models for force constants and deep core states.

Professor Lucovsky is a Fellow of the American Physical Society and the American Vacuum Society and a member of the Solid State Sciences Panel of the National Academy of Sciences. Also, he is Editor in Chief of the Journal of Vacuum Science and Technology.

Revolutionary High Temperature Superconductors

By Donald Gubser
Naval Research Laboratory

In October 1986, scientists at IBM Zurich reported that a material which they had been studying appeared to become superconducting (i.e. lose all traces of electrical resistance) at temperatures as high as 30K (−243 C). Confirmation on this report was provided by scientists from Japan who reported their findings at a Materials Research Society meeting on 5 December in Boston. Research on these materials has exploded since these initial reports and the temperature at which superconductivity occurs has recently been reported at 100 K (−173C) by researchers at the University of Houston.

Superconductivity was discovered in 1911 in Mercury with a superconducting transition temperature T_c of 4K. Over the years, T_c in has moved up until, prior to the recent discovery, the record T_c was 23K in the compound Nb_3Ge. These new materials represent a quantum jump in T_c and will have as much (or more) impact on science and technology as the development of the microscopic theory of superconductivity or the discoveries of the Josephson effect and of high magnetic field superconductors.

These results are truly revolutionary. They mean that scientists must reexamine many of their long held concepts about the mechanisms producing superconductivity as well as the materials where it is most likely to occur. The material is a metallic ceramic oxide composed of the elements Lanthunum, Copper, Oxygen, and small amounts of either Barium, Strontium, or Calcium. The arrangement of atoms in the material as well as the unusually high superconductivity suggest that new mechanisms may produce a host of novel physical properties in these materials. The normal interaction which produces superconductivity is a coupling of the electrons in a metal with the vibrations of host atoms. Other types of interactions which might enhance superconductivity in these materials are coupling between the free electrons and plasma oscillations of this same electron system. Similarly the layered structure of the material suggest that two-dimensional effects may be responsible for the high superconductivity.

From a technological viewpoint, the new materials will permit applications of superconductivity with much simplified refrigerations systems. Applications range from large superconducting magnets used in such systems as: fusion energy reactors, electrical motors, energy storage, medical analysis (MRI) and elementary particle accelerators (SSC); to smaller scale electronic systems such as: magnetometers for medical or magnetic anomally detection purposes, detectors of electromagnetic radiation, and high speed digital circuitry. These and many more superconducting applications will now become technologically and economically viable options for a variety of uses. In many cases superconductivity is the only available option for an emerging technology. These new materials will speed the development of all superconductivity applications due to easing of the refrigeration requirements.

The Navy has many uses for superconductivity, from motors for ship propulsion, to magnetometers for underwater ocean surveillance, to detectors of electromagnetic radiation. Research sponsored by the Office of Naval Research and the Office of Naval Technology has fostered development in superconductivity for many years primarily in the area of superconductive electronics. The Naval Research Laboratory has had strong research programs to develop a fundamental understanding of the materials and phenomena of superconductivity and on the development of superconducting materials for both magnet and electronic applications. Naval research and development centers such as the Naval Ship Research Development Center and the Naval Coastal Systems Center are developing systems applications for superconductivity such as ship propulsion and non acoustical magnetic detection systems. The new superconducting materials will have significant impact on all these research and development programs.

Scientists at the Naval Research Laboratory are developing these new superconducting materials and studying a variety of processing techniques to further improve their properties. The materials are made by mixing oxides and carbonates of Lanthanum, Barium, Strontium, and Copper in a platinum crucible and reacting at temperatures near 1000C to form the desired compound. This material is then pressed into shape and sintered at 1000C to form bulk samples. The samples are then tested for superconductivity by cooling in a special dewar designed to measure the electrical resistance as a function of temperature. The compounds made at NRL have superconducting transitions temperatures over 40K and are being used to test a variety of properties. Similarly, NRL theorists are actively engaged in efforts to understand the materials from a microscopic point of view.

A major initiative is now underway within the Navy to understand and develop these materials for naval application. Once developed, superconductive systems are expected to play a dominant role in the high tech navy of the future.

Biography

Dr. Donald Gubser is Head of the Metal Physics Branch and the Condensed Matter and Radiation Sciences Division at the Naval Research Laboratory (NRL), Washington, D.C. His publications and research are in the field of superconductivity for which he is the point of contact at NRL. He recently was co-organizer of the High Temperature Superconducting Symposium held in Anaheim, California, under the auspices of the Material Research Society and co-editor of the symposium proceedings.

Research Notes

New Excimer Laser Concept

Dr. Bernard Wexler of the Naval Research Laboratory (NRL), reports the conception, development, and successful laboratory-testing of a large-aperture, discharged-pumped excimer laser design which is expected to improve the efficiency and energy of such lasers. This research is funded by the Office of Naval Research.

Rare gas excimer lasers, such as argon fluoride, krypton fluoride, and xenon chloride have become useful in scientific research and could be applied to medical use, materials processing, and military applications.

Excimers are molecules that exist only in their excited states. Large populations of these molecules can be created (pumped) efficiently by passing electron beams or electric discharges through gas mixtures containing the appropriate parent atoms and molecules. Electron-beam pumping has been used for very high energy lasers. Discharge pumping, which has the potential for high efficiency and a high pulse repetition rate, has been used for smaller devices, including many commercial lasers.

Dr. Wexler reports he has been using a concept originated by Mr. John D. Shipman, Jr., a consultant and former employee at NRL (presently employed by Sachs/Freeman Association, Inc.) to demonstrate that the inductance of these discharge lasers, particularly those with apertures 10 centimeters in diameter and greater, can be reduced by a factor of two or more. The technique uses careful geometric shaping of the electric fields of the laser head, so that flashover of the discharge along the walls is avoided. This flashover was previously avoided by keeping the walls farther away from the discharge region, significantly increasing the inductance of the laser head.

Because the inductance adversely affects the rise time of the current pulse and consequently the efficiency of the laser, the use of the concept will increase the practical maximum size, and therefore, the output energy of discharged-pumped excimer lasers.

Alternatively, devices of a given energy can be constructed in a smaller volume and the pulse length decreased, due to the low inductance, which can increase the instantaneous power available. Dr. Wexler cautions that the concept has been demonstrated for single pulse lasers only, but he believes that it should be possible to extend the use of the technique to repetitively pulsed systems, which require gas flow.
(B. Wexler, NRL)

Cold Temperatures Improve Semiconductors

Scientists at the Naval Research Laboratory (NRL) are studying an emerging technology known as *cold electronics* to improve the performance of semiconductor devices and microchips. This approach uses extremely low temperatures—much lower than that of dry ice (minus 70 degrees Celsius)—rather than decreased dimensions for increasing the speed and improving the performance of the devices. Cold electronics could have widespread applications in the Fleet as the need increases for faster and more dense electronic chips.

The usual approach for achieving high speed and a large number of devices on a chip has been to progressively reduce the dimensions of each device and to place them closer and closer together. However, as the dimensions of the features of the devices are shrunk below about one-half micrometer (about one-onehundredth the diameter of a human hair), they become extremely difficult to fabricate, and it becomes very difficult to make many devices all working to specification.

Dr. Martin Nisenoff of NRL's Electronics Technology Division reports that these problems can be circumvented by cooling devices and chips to the temperature of liquid nitrogen (about minus 200 degrees Celsius). In this temperature range, the velocity of the electrons moving in the devices is three to ten times faster than at room temperature. Because the speed of the electrons is increased, they can travel over a longer distance in the same amount of time. Thus, larger devices using cold electronics can achieve the same speeds as smaller room-temperature devices. This avoids the fabrication problem and enables the production of devices that have a high yield.

For most materials used to connect devices on a chip, the resistance of the metallic "wires" decreases as the operating temperature is reduced below room temperatures. This reduction in the electrical losses on the chip allows the devices to be more closely packed for chips cooled to very low temperatures compared with those operated at room temperature.

Cooling of electronic devices to cryogenic temperatures is not new. Nisenoff explains that cooling has been successfully used for more than 20 years by radio astronomers who have used radio receivers cooled to liquid helium temperatures (about minus 269 degrees Celsius) to study the cosmic background of the universe.
(M. Nisenoff, NRL)

Immune System Hormones Act Directly on the Stress Response of the Brain

A recent "Science" article (29 November 85) by ONR investigators revealed that hormones secreted by macrophages, key cells in the immune system, directly activate the pituitary gland in the brain. The pituitary has long been known to respond to signals from the hypothalamus in the brain to release a hormone called ACTH, which in turn stimulates the adrenal gland over the kidney to secrete steroid hormones; steroids are involved in gene activation and a broad range of adaptive responses, but in excess can have maladaptive actions. Steroids are generally considered primary mediators of responses to stressful events. The findings by this group at the University of Texas Medical Branch in Galveston, headed by Dr. J. E. Blalock, clearly demonstrate that macrophage hormones, specifically interleukin-l and hepatocyte-stimulating factor, are equally potent, or more so, as the hypothalamic hormones CRF and arginine vasopressin. This work demonstrates an unexpected but potentially very important signalling process going from the immune system to the brain and supports the new concept that the immune system serves as an extension of the central nervous system.
(J. A. Majde, ONR)

Superconductive Detector Used to Verify New General Relativity Prediction

Using two Josephson junctions, vertically separated by about 10 cm. Professor James Lukens of the State University of New York has verified a new relativistic prediction of a potential difference variation in a gravitational field. For two years Lukens has been attempting to verify the so-called gravitational "red shift." In these preliminary experiments, he connected a pair of vertically separated Josephson junctions in parallel to form a dc SQUID loop which was phased locked to a single voltage by a common microwave source. Due to the gravitational "red shift," the voltages across the junction should differ by Delta $V = Vgh/c^2$ which is about 2.3 X 10^{-21} volts.

Recently, the sensitivity of the experiment has been increased by about 100 times from that achieved two years ago. A resolution 10 times greater than the voltage difference of 2 X 10^{-21} volts due to the "red shift" in the phase-locking radiation is routinely achieved. A most surprising result is observed. Lukens unambiguously measures the net loop voltage which turns out to be less than 5% of the difference in junction voltage due to the "red shift." This requires the existence of an additional voltage difference in the SQUID loop having an equal and opposite sign to that of the junctions.

Such an effect, based on general relativity, has recently been predicted. It can be understood qualitatively as follows: a loop of superconducting wire carrying a current runs vertically in a gravitational field. Observers at different heights will measure different currents; however, since charge is conserved and their local clocks run at different rates due to the differing field. Thus $I = dQ/dt$ will vary with height along the wire. Now, imagine breaking the loop at some height, inserting a resistor and measuring the voltage drop. If this experiment is repeated at different heights using the same resistor, then different voltages must be measured since the local observer measures different currents.

Lukens believes that the observation of this effect is at least on a par with the "red shift" as a test of general relativity. Anandeen, who predicted this new effect, claims that it represents an even stronger test since it is the first test of relativity theory involving charged particles.
(R. Brandt, ONR)

Methane Utilization in Deep Sea Mussels

In research on life forms associated with deep sea hot vents, large numbers of clams and mussels have been noted, prompting questions of where these and related forms obtain their food. Recently, two ONR contractors, R. Mitchell of Harvard University and M. E. Lidstrom of the University of Wisconsin at Milwaukee, reported in the journal *Nature* on evidence for bacterial symbiosis as a food source. Bacteria living within large cells in the thick, fleshy gills of deep sea mussels apparently use methane dissolved in the sea as the energy source to convert the carbon in CO_2 into hydrocarbon compounds (i.e., food). The bacteria are chemolithautotrophic: they chemically use the energy in mineral compounds (methane) to produce their own food (autotrophic) similar to the way that green plants produce their own food by using sunlight as the energy source (photosynthesis). The research on this new example of animals capable of using methane as a food source explains how they can do it: the bacteria in their gills actually provide the food to the mussels in this symbiotic relationship.
(B. Zahuranec, ONR)

New Technique for Optical Information Storage Reported

The first observation of a phenomenon called, "two-color, photo-gated spectral hole burning" in an organic material has been reported by Drs. W. E. Moerner, IBM Almaden Research Laboratory, M. Geherty, University of Munich, and co-workers in Chemical Physics Letters. This technique is being investigated for potential application for optical information storage in optical computers. This technique allows non-destructive reading of stored information a desirable quality for retrieval of information from optical storage systems. This fundamental research will provide the scientific base for fast and reliable optical computers for various Navy applications and is supported jointly by Office of Naval Research and IBM Corporation.
(H. Guard, ONR)

Diamond Films

Professor Rustum Roy at Pennsylvania State University has succeeded in synthesizing diamond films. The films are produced from a microwave plasma (2.54 GHz, a gas mixture of methane and hydrogen). Films up to 0.5 micrometer thick have been produced so far. The presence of atomic hydrogen in the plasma is believed to be the key to the growth of the diamond phase, though the films do not contain an appreciable amount of hydrogen. There is evidence that changing the conditions so as to incorporate more hydrogen in the film could produce material having a hardness *greater* than that of single crystal diamond. Process conditions having primary importance to results are: (1) the relative proportions of the methane and hydrogen; (2) the substrate temperature; and (3) the position of the substrate relative to the plasma.

Such films, because of their high hardness and optical properties, would be ideal protective coatings in a wide variety of applications, e.g. windows for sensors. This approach to the synthesis of diamond without the use of high pressure had been pioneered by the Setaka group at NIRIM, Tsukaba, Japan. Current efforts are focussing on understanding how to get faster film growth.
(D. Polk, ONR)

NO POSTAGE
NECESSARY
IF MAILED
IN THE
UNITED STATES

BUSINESS REPLY CARD

FIRST CLASS PERMIT NO. 12503 WASH., D.C.

POSTAGE WILL BE PAID BY DEPARTMENT OF THE NAVY

Editor
Code OOPARI
Office of the Chief of Naval Research
Arlington, VA 22217-5000

DEPARTMENT OF THE NAVY
OFFICE OF NAVAL RESEARCH
ARLINGTON, VA 22217-5000

OFFICIAL BUSINESS
PENALTY FOR PRIVATE USE, $300

POSTAGE AND FEES PAID
DEPARTMENT OF THE NAVY
DoD-316

THIRD CLASS

Important Renewal Notice

(Does not apply to paid subscription readers)
(Send entire back cover, folded as indicated, with mailing label attached)

FOLD FOLD FOLD

Readership Survey

Navy publications and printing regulations require that all mailing lists be verified at least once a year to identify incorrect addresses and addressees who no longer qualify for free distribution.

Please indicate if you want to continue receiving *Naval Research Reviews* and add any comments you may have about the publication. We will consider these comments in planning future issues. Also, indicate any change of address below the label, and make sure the label is returned with this survey. Fold this sheet and staple to reveal NRR address.

Addressees whose response does not reach the *Naval Research Reviews* Editor by December 1, 1987, will be removed from the mailing list.

Please Complete the following

1. ☐ I want to continue receiving Naval Research Reviews.
2. ☐ Please remove me from the mailing list.

Comments: